Citrus relatives exhibit natural variation in perception and response magnitude to microbial features

Jessica Trinh*[1], Tianrun Li*[1], Jessica Y. Franco*[1], Tania Y. Toruño*[1], Danielle M. Stevens*[1], Shree P. Thapa[1], Justin Wong[1], Rebeca Pineda[2], Emmanuel Ávila de Dios[2], Tracy L. Kahn[2], Danelle K. Seymour[2], Chandrika Ramadugu[2], Gitta L. Coaker[†1]

[1] Department of Plant Pathology, University of California, Davis, CA, USA

[2] Department of Botany and Plant Sciences, University of California, Riverside, CA, USA

[†] Corresponding author

* These authors contributed equally to the work.

Abstract

Although much is known about the responses of model plants to microbial features, we still lack an understanding of the extent of variation in immune perception across members of a plant family. In this work, we analyzed immune responses in *Citrus* and wild relatives, surveying 86 Rutaceae genotypes with differing leaf morphologies and disease resistances. We found that responses to microbial features vary both within and between members. Species in two subtribes, the Balsamocitrinae and Clauseninae, can recognize all tested microbial features (flg22, csp22, chitin), including one from *Candidatus* Liberibacter species ($csp22_{CLas}$), the bacterium associated with citrus greening disease aka Huanglongbing. Chitin perception is widespread among Rutaceae genotypes. We were able to characterize a homolog of the *Arabidopsis* LYK5 receptor in 'Tango' mandarin that is capable of conferring chitin perception. These findings shed light onto the diversity of perception of microbial features and highlight genotypes capable of recognizing polymorphic microbial features whose receptors have promise for transfer to susceptible varieties.

Keywords: plant immunity, MAMPs, citrus, Rutaceae, citrus Huanglongbing

Introduction

The perception of microbial features has typically been assessed by using a single or few plant genotypes to make conclusions about microbial perception. Recognition of conserved features of pathogens, known as microbe-associated molecular patterns (MAMPs), activates the plant immune system. MAMPs can be proteinaceous or structural pathogen features and are

perceived by plant immune receptors. While many studies are focused on the immune responses of one representative genotype, responses to MAMPs exhibit variation within and between related species. For example, different genotypes of *Arabidopsis thaliana* contain FLS2 homologs that vary in binding specificity to an epitope of bacterial flagellin, and low binding specificity correlated with high bacterial proliferation (Vetter *et al*. 2012). Epitopes from three bacterial MAMPs were differentially recognized across heirloom tomato genotypes, indicating the diversity in immune responses within a group of closely-related plants (Veluchamy *et al*. 2014). The extent of natural variation in immune responses to microbial features still remains largely unexplored.

The Rutaceae plant family contains ~2100 species with worldwide distribution, including the agriculturally important genus *Citrus* (Kubitzki *et al.* 2011). Citrus is the most extensively produced fruit crop in the world with 124.246 million tons of fruit produced in 2016 (Zhong & Nicolosi 2020). In the United States, the 2019 - 2020 growing season yielded a value of production of about 3.4 billion dollars for citrus products (USDA 2020). Florida alone is the second largest producer of orange juice in the world behind Brazil, its citrus economy contributing billions of dollars to the state Gross Domestic Product (Hodges & Spreen 2012). While oranges constitute more than half of worldwide citrus production, other relevant citrus products include tangerines, limes, lemons, and grapefruits (Liu *et al.* 2012). These different varieties of cultivated citrus are members of the genus *Citrus* in the family of Rutaceae, which contains several non-cultivated relatives of *Citrus* (Wu *et al.* 2018). Several systems of classification exist; in this study, we followed the classification of Swingle and Reece (1967). Rutaceae contains six subfamilies (Appelhans *et al.* 2021) and the subfamily to which citrus belongs, Aurantoideae, contains two tribes: Citreae and Clauseneae (Morton 2009). The Citreae contains three subtribes, which are Citrinae, Triphasiinae, and Balasmocitrinae. Clauseneae contains three subtribes: Micromelinae, Clauseninae, and Merrillinae (Nagano *et al*. 2018). The Citrinae subtribe contains all cultivated citrus genotypes and is the most important group in the family Rutaceae (Swingle and Reece 1967).

Cultivated citrus is a perennial crop that is vegetatively propagated through grafting (Castle 2010, Caruso *et al*. 2020). While these asexual propagation methods maintain the desired combinations of traits in commercial cultivars, they prevent the exchange of genetic material (Uzun & Yesiloglu 2012, Wang *et al.* 2017). Because of this, crops that are primarily propagated asexually are susceptible to devastating impacts from newly introduced citrus diseases.

Cultivated citrus varieties are susceptible to a variety of microbial pathogens including bacteria, filamentous pathogens, and viruses. Breeding efforts often focus on developing rootstocks with resistance to these pathogens to fend off disease in the clonally propagated scion. Examples of citrus diseases with a significant impact on citrus production include citrus Huanglongbing (HLB) (Bove *et al.* 2006, Wang 2019), citrus canker (Ference *et al.* 2018, Das 2003), citrus variegated chlorosis (Colleta-Filho *et al.* 2020), as well as fruit and root rots (Jaouad *et al.* 2020).

To protect themselves from pathogens, plants have evolved multiple defense mechanisms including MAMP perception. MAMPs can be proteinaceous, such as the flagellin or cold shock protein of bacteria (Wang *et al.* 2016) or not, such as bacterial lipopolysaccharide or fungal chitin (Newman *et al*. 2013). To detect MAMPs, plants possess pattern-recognition receptors (PRRs) on the surface of their cells. PRRs include receptor-like kinases (RLKs) and receptor-like proteins (RLPs). RLKs consist of an extracellular domain, a transmembrane domain, and an intracellular kinase domain, whereas RLPs lack the intracellular kinase domain. Examples of PRR extracellular domains include leucine-rich repeats (LRRs), lysine motifs (LysM), and lectin domains, among others (Ngou *et al.* 2022). Binding of the MAMP to the PRR often results in heterodimer formation with a coreceptor to activate downstream signaling responses and host defenses ultimately leading to MAMP-triggered immunity (MTI). Hallmarks of MTI activation include apoplastic reactive oxygen species (ROS) production, intracellular mitogen-activated protein kinase (MAPK) activation, and global transcriptional reprogramming (Saijo *et al.* 2017, Cuoto & Zipfel 2016, Bigeard *et al*. 2015).

Extensive research has been performed in the last few decades to reveal PRRs that perceive various MAMPs in model and crop plants (Ngou *et al.* 2022). Some well-characterized receptors include: the *Arabidopsis* FLS2 receptor for a 22-amino acid epitope of bacterial flagellin (Gómez-Gómez & Boller 2000), the *Arabidopsis* LysM domain receptor (LYK4/5) of chitin (Miya *et al.* 2007, Cao *et al.* 2014), and the tomato (*Solanum lycopersicum*) CORE receptor for a 22-amino acid epitope of bacterial cold shock protein (Wang *et al.* 2016). However, more work needs to be done to discover novel immune receptors in tree crops and other non-model plants. Genome mining for citrus LRR-RLKs suggest that there are receptors capable of mediating host-pathogen interactions. Although RLKs have been predicted in the *C. sinensis* and *C. clementina* genomes, no immune receptors have been functionally validated in citrus (Magalhães *et al* 2016, Dalio *et al*. 2017). Previous studies have identified citrus FLS2 homologs, one of which is induced in response to bacterial flagellin (Shi *et al.* 2016). In addition,

one Liberibacter-specific MAMP for the bacterial protein pksG was recognized in three out of 10 citrus genotypes (Chen *et al.* 2020).

For this study, we have examined the responses of several genotypes encompassing both cultivated citrus and wild relatives to different microbial features. Our objective was to better understand the landscape of immune perception within the Rutaceae family. After identifying genotypes capable of perceiving a broad range of microbial features using a ROS-based high-throughput screen, we further validated these responses by assessing MAPK activation. Most of our selected genotypes, including those from cultivated citrus, can perceive chitin and chitin receptor homologs are present across higher plants, suggesting that chitin perception is derived from an ancient receptor. We were able to isolate a homolog of the *Arabidopsis* chitin receptor *LYK5* from cultivated citrus and demonstrate its functionality in a non-host species. We also uncovered citrus relatives that can perceive a conserved feature of *Candidatus* Liberibacter asiaticus (*C*Las), the bacterium associated with citrus Huanglongbing. These results highlight the importance of studying immunity in wild relatives, especially to identify potential genotypes with immune mechanisms that can be transferred to disease-susceptible cultivars.

Results

Members of the Rutaceae family exhibit diversity in the perception of and magnitude of response to microbial features

To investigate the immune response capabilities of members of the Rutaceae family, we screened 86 genotypes for the perception of three common microbial features: chitin, flg22, and csp22. These genotypes were samples from the Givaudan Citrus Variety Collection (GCVC) at the University of California, Riverside. The GCVC is one of the most comprehensive collections of citrus diversity, including over 1,000 accessions that span the genus *Citrus* and related genera. This study includes representatives spanning known subtribes in Rutaceae, including both cultivated citrus and wild relatives. In total, we screened individuals from two subfamilies (Aurantoideae and Zanthoxyloideae) and representative taxa from all six subtribes of Aurantoideae, comprising over 30 different genera. The majority of selected genotypes fall within the Citrinae subtribe (56 genotypes), which includes the cultivated citrus types. Genotypes are referred to by their common name, if available, with the corresponding scientific name and accession number in Table **S1**. To measure the ROS output of multiple genotypes, we have optimized a plate-based assay for high-throughput screening of leaves from both

seedlings and mature trees. The genotypes we screened exhibit a variety of different leaf, branch, and fruit morphologies (Table **S1,** Fig. **1b**). A luminol analog, L-012, chemically reacts with horseradish peroxidase and ROS to produce light, which is measured by the plate reader as relative light units (RLUs). RLUs from a ROS burst can be plotted as a curve over time, area under the curve, or in this case, the peak of ROS production (max RLU). The results from the ROS-based assay are presented as an average of max RLUs across multiple independent experiments in Figure **1a.**

The landscape of immune perception varied across genotypes, with the strength of the response to each elicitor segregating across members from most surveyed tribes (Fig. **1a**). There were differences in the proportion of genotypes responding to each elicitor. For example, nearly all genotypes screened are capable of perceiving chitin (75 out of 86 genotypes), but less than half of the screened genotypes are capable of perceiving flg22 (40 out of 86 genotypes). More than half of the screened genotypes (45 out of 86 genotypes) are capable of perceiving csp22, but there appears to be no clear relationship between the taxonomic groups and csp22 perception. Because of widespread chitin perception across cultivated citrus and wild relatives, it is likely that these genotypes share a conserved chitin receptor and maintained the ability to perceive chitin across eight million years of evolution (Gmitter and Hu 1990, Xie *et al.* 2013). There is substantial segregating variation in MAMP perception across tribes. For example, within the Citrinae tribe, 'Tango' mandarin (*Citrus ×aurantium* L.*)* can perceive all three MAMPs, but kumquat (*Fortunella hindsii* (Champ. ex Benth.) Swingle) cannot perceive any of the three. Twenty-four genotypes are capable of perceiving all three MAMPs in addition to 'Tango' mandarin. Closely related genotypes, such as 'Tango' mandarin and 'Lee' mandarin, also have varying responses to MAMPs: 'Tango' mandarin responds to all three MAMPs, but 'Lee' mandarin can only perceive chitin. Genotypes capable of responding to all three MAMPs are members belonging to the subtribes Balsamocitrinae, Clauseninae, Citrinae, and Triphasiinae (Fig. **1a**). This variation may be the result of differences at the receptor level or in downstream signaling components.

Rutaceae genotypes vary not only in their ability to perceive MAMPs but also in the magnitude of ROS production (Figs. **1, 2**). The magnitude of ROS production as a result of chitin, flg22, or csp22 induction occurs across tribes as well as within members of a tribe. Although the majority of the screened Rutaceae genotypes are capable of perceiving chitin, some genotypes produce an average max RLU of less than 1,000, while others produce an average max RLU well over

10,000 in response to chitin. To categorize the strength in responses, 25th and 75th quartiles were computed for each MAMP and cutoffs were used. Figure **2a** shows examples of “weak” (25th percentile or below), “medium” (between the 25th and 75th percentiles), and “strong” (75th percentile or greater) responders. Across tribes, we see that members of the Triphasiinae tribe, such as the trifoliate limeberry, are strong responders to chitin, whereas some members of the Balsamocitrinae subtribe, such as the Chevalier’s Aeglopsis, are either weak or medium responders (Fig. **2b**). Within the Citrinae tribe, ‘Tango’ mandarin and Uganda cherry-orange are strong responders to flg22, but ‘King’ tangor is a weak responder to flg22 (Fig. **2c**). Trifoliate limeberry is also a strong responder to csp22 (Fig. **2d**). The data showcase strong and weak responders to MAMPs that are spread out within and between taxonomic groups.

In addition to the production of ROS, other common immune responses include MAPK activation, defense gene expression, and callose deposition. One of the challenges of studying Rutaceae is that many of the genotypes in this study do not have their genomes sequenced, making primer design for defense gene expression experiments difficult. Additionally, the thick, waxy leaves of citrus plants make it challenging to visualize callose deposition via microscopy. MAPKs are highly conserved across eukaryotes (Meng and Zhang 2013), making them viable immune markers to study MAMP responses in a variety of genotypes. MAPKs are phosphorylated upon MAMP perception, which can be detected via Western blot. In order to determine if the ROS production data is consistent with activation of other immune responses, we analyzed a subset of Rutaceae genotypes from three different subtribes (Balsamocitrinae, Clauseninae, and Citrinae) for PTI-induced MAPK activation. Background MAPK phosphorylation was not observed in the water infiltration for ‘Midknight Valencia’ orange, but MAPK phosphorylation was induced at 10 min after water infiltration in ‘Frost Lisbon’ lemon, Orange jasmine, and Uganda powder flask (Fig. **3b**). These results correspond to observations in other species, where MAPK phosphorylation can also be weakly induced in response to water or buffer treatment but is strongly phosphorylated in response to immune activation (Zhang *et al.* 2013). ‘Midknight Valencia’ orange is only able to respond to chitin based on ROS results. Similarly, ‘Midknight Valencia’ orange only exhibits MAPK phosphorylation upon chitin treatment, where a strong band appears at 10 and 20 minutes after induction with chitin compared to the water treatment. ‘Frost Lisbon’ lemon responds to chitin, flg22, and csp22 based on ROS results, but only induces sustained MAPK phosphorylation in response to chitin and flg22 treatment. For Orange jasmine and Uganda powder flask, two non-Citrinae genotypes, we can observe ROS production in response to chitin, flg22, and csp22. While chitin induced MAPK

phosphorylation was robust in both genotypes, flg22 perception was only observed in two out of four MAPK trials for the Uganda powder flask. Interestingly, we were not able to detect MAPK phosphorylation for csp22 in genotypes that can respond to this MAMP in ROS assays. In Arabidopsis, downstream immune responses can vary in presence and magnitude depending on receptor type (Wan *et al.* 2018). Taken together, these data indicate that Rutaceae genotypes can respond to MAMPs by inducing ROS and MAPK activation for flg22 and chitin.

Cultivated citrus genotypes contain functional chitin receptor homologs

Multiple plant families are able to perceive chitin. In *Arabidopsis*, chitin is perceived by two LysM domain receptor-like kinases (LYK4/5) and the co-receptor CERK1 (Miya *et al.* 2007, Cao *et al.* 2014). Knockouts of both *lyk4/5-2* or the co-receptor *cerk1* do not respond to chitin (Cao *et al*. 2014). The LysM domain and chitin binding (Y128 and S206) residues are conserved in 'Midknight Valencia' orange, 'Washington navel' orange, and 'Tango' mandarin (Fig. **S2b-c**). Homologs of *Arabidopsis* CERK1 have been found in the monocots wheat (*Triticum aestivum*) and rice (*Oryza sativa*) (Lee *et al.* 2014, Miyata *et al.* 2014, Shimizu *et al.* 2010). In our experiments, chitin is widely perceived across members of the Rutaceae, including both cultivated citrus types and wild relatives (Fig. **1a**), indicating that chitin perception is likely derived from a conserved receptor. Therefore, we sought to further investigate the presence of *LYK5,* the major chitin receptor (Xue *et al.* 2019, Erwig *et al*. 2017, Cao *et al.* 2014), and *CERK1* across the plant kingdom. Members of the LYK family are known to be involved in perception of multiple features including Nod factor, peptidoglycan, and chitin, highlighting the importance of accurately predicting CERK1 and LYK5 orthologs (Antolín-Llovera *et al.* 2014). To identify and assess the conservation of *Arabidopsis thaliana* $LYK5_{At}$ and $CERK1_{At}$ across a variety of eudicots and monocots, we used an approach based on homology, phylogeny, and hidden Markov models. Mid-rooted maximum likelihood trees show broad conservation of LYK5 and CERK1, with 41% of genotypes possessing multiple $LYK5_{At}$ homologs and 51% possessing multiple $CERK1_{At}$ homologs (Fig. **4a**). There are two predominant LYK5 clades, a monophyletic monocot clade and a polyphyletic dicot clade including members from the Brassicaceae*,* Fabaceae*,* Malvaceae, and Rutaceae families. Interestingly, $LYK5_{At}$ homologs from members of the Solanaceae family were filtered out before tree building as they were closer to $LYK4_{At}$ than $LYK5_{At}$. CERK1 displayed two major clades split by homologs from eudicots and monocots. Despite the diversification that can be found within the ectodomain of LYK5 and CERK1

homologs when compared against *Arabidopsis*, residues in LYK5$_{At}$ which are known to directly bind to chitin are conserved (Fig. **4b-c**) (Cao *et al.* 2014).

Additional citrus LYK5 members for Australian finger lime, 'Rio Red' grapefruit, 'Frost Lisbon' Lemon and Eremolemon were PCR amplified, sequenced, and plotted on the phylogeny. LYK5 homologs within the Citrinae tribe exhibit low copy number and diversification, predominantly clustering in a single subclade (Fig. **4a**). Only clementine and 'Midknight Valencia' orange (*Citrus ×aurantium* L.) carried an additional copy of LYK5, which is more closely related to those from cotton and durian (Fig. **4a**). We attempted to PCR amplify additional CERK1 homologs in Citrinae but were only able to amplify from 'Rio Red' grapefruit. Within eudicots, citrus CERK1 homologs are polyphyletic and both clementine and 'Midknight Valencia' orange carry multiple homologs (Fig. **4a**)**.** Ectodomains of citrus receptor homologs were compared, revealing a bimodal distribution for LYK5 and CERK1 and high amino acid similarity within citrus subclades (Fig. **4b**).

The LysM domain is critical and required for chitin binding. However, the ability to predict these domains computationally is not always congruent (Shimizu *et al.*, 2010). Standard domain prediction software Interproscan of LYK5$_{At}$ and CERK1$_{At}$ failed to predict the correct number of LysM domains (data not shown). Therefore, we used both homology and hidden Markov models to predict LysM domains and found an incongruence between the number of domains predicted (Fig. **4a**). Therefore, while we can confidently predict potential chitin receptor candidates, functional validation may still be required.

Although most cultivated citrus genotypes can perceive chitin, there is still a wide range for the magnitude of the ROS response (Fig. **1a**). 'Washington navel' orange (*Citrus ×aurantium* L.) is a type of sweet orange and many modern type III mandarins are often derived from hybrids of sweet oranges and other mandarin types (Wu *et al.* 2018). Both 'Washington navel' orange and 'Tango' mandarin contain homologous LYK5 alleles in syntenic genetic regions that are highly similar to each other (99.6% amino acid similarity, Fig. **5c, S2a**). These *LYK5* homologs are also expressed similarly in both genotypes using qPCR (Fig. **5d**). However, 'Tango' has a stronger response to chitin, with a five-fold stronger ROS burst (Fig. **5a**). Chitin also activates MAPKs in both 'Washington navel' and 'Tango', though the magnitude of the response varies (Fig. **5b**). 'Tango' was a stronger responder than 'Washington navel' in two experiments and an equal responder in two experiments. To validate the functionality of the 'Tango' LYK5, we

complemented *lyk4/lyk5-2 A. thaliana* with the 'Tango' LYK5 (referred to as $LYK5_{TM}$) or *Arabidopsis* allele ($LYK5_{At}$). Two independent *A. thaliana* transgenic lines expressing $LYK5_{TM}$ as well as $LYK5_{At}$ regain the ability to produce ROS in response to chitin treatment (Fig. **6a**). Immunoblot analyses against the HA epitope tag verified protein expression of all transgenes. We were able to further confirm the functionality of this receptor with additional immune assays. Both $LYK5_{TM}$ as well as $LYK5_{At}$ complementation lines exhibited MAPK phosphorylation upon chitin treatment (Fig. **6b**). Taken together, we have demonstrated that cultivated citrus can respond to chitin, possess LYK5 and CERK1 homologs, and $LYK5_{TM}$ can function as a chitin receptor in *Arabidopsis*.

Members from the Citrinae, Balsamocitrinae, and Clauseninae subtribes are capable of perceiving csp22 from an important citrus pathogen

In tomato, the CORE receptor-like kinase perceives csp22, generating resistance to the bacterial pathogen *Pseudomonas syringae pv. tomato* DC3000 when expressed in *A. thaliana* (Wang *et al.* 2017). The closest *Nicotiana benthamiana* homolog of tomato CORE is able to induce ROS production in response to csp22 treatment after transient expression (Wang *et al*. 2016). In order to gain insight into candidate citrus csp22 receptors, we analyzed citrus genomes for the presence of CORE receptor homologs. However, the closest citrus homolog of either *Nicotiana* or *Solanum* CORE receptors had several polymorphisms in the ectodomain (Fig. **S5d-e**). Expression of the receptor recognizing csp22 is developmentally-regulated and expressed in flowering *Nicotiana benthamiana* and tomato (Saur *et al.* 2016, Wang *et al.* 2016), which makes it possible to use *Agrobacterium* transient expression to investigate CORE in young *Nicotiana benthamiana*. We investigated the CORE homologs from 'Frost nucellar Eureka' lemon and 'Washington navel' orange, which are responsive to csp22. When these CORE homologs were heterologously expressed in 30 day-old *Nicotiana benthamiana*, they failed to confer csp22 responsiveness, in contrast to expression of *NbCORE*. All CORE proteins were expressed by immunoblot analysis (Fig. **S5c**)**.** These data suggest that Rutaceae possess an independently derived csp22 receptor.

Proteinaceous MAMPs are often conserved across pathogens. However, due to strong selection pressure, some pathogens have evolved immunogenic epitopes that cannot be perceived, while still retaining the presence of the entire protein (Cheng *et al.* 2021). The csp22 epitope from *C*Las ($csp22_{CLas}$) contains several polymorphisms when compared to the canonical csp22

sequence (Fig. **7a**). Therefore, we investigated if there were members of the Rutaceae family that could perceive csp22$_{CLas}$ (Fig. **7b**). The vast majority of Rutaceae genotypes that can respond to canonical csp22 cannot perceive csp22$_{CLas}$ using ROS production as an output. Notably, members from the Balsamocitrinae and Clauseninae subtribes can perceive both canonical csp22 and csp22$_{CLas}$, such as Uganda powder-flask and *Clausena harmandiana*. There is one member of the Citrinae tribe, the 'Algerian clementine' mandarin, that perceives csp22$_{CLas}$, but not canonical csp22. *Clausena harmandiana* is able to induce MAPK phosphorylation in response to csp22$_{CLas}$ compared to the non-responding genotype 'Midknight Valencia' orange (Fig. **7d**). Genotypes that respond to csp22$_{CLas}$ also exhibited some level of reduced symptomology to HLB disease in field trials with mature trees (Fig. **S4,** Ramadugu *et al.* 2016). Data generated from our high-throughput ROS screens in members of Rutaceae reveal members that can be used to identify novel receptors for transfer to *C*Las-susceptible citrus cultivars.

Discussion

Here, we have investigated variation in MAMP perception within a family of related woody genotypes to determine the landscape of perception in citrus and citrus relatives. Variations in MAMP perception have been noted within genotypes of the same species, such as in tomato (Roberts *et al.* 2019) and in *Arabidopsis* (Vetter *et al* 2012). Even in close relatives, the perception of a potent immune elicitor such as flg22 varies widely (Veluchamy *et al*. 2014). Much more diversity remains to be discovered by analyzing multiple genotypes. Perennial genotypes like citrus are largely unexplored due to long lifespans lengthening the time required to perform experiments, large field or greenhouse space required to grow tree crops, reduced access to diverse genotypes, and a lack of genomic resources.

There are multiple potential reasons why studies have observed variation in MAMP perception among related species. While some species may contain the same receptor homolog, the presence of the homolog does not always correlate with strong MAMP perception (Vetter *et al.* 2012, Trdá *et al.* 2013). In this study, the LYK5$_{At}$ homologs in 'Washington navel' orange and 'Tango' mandarin only differ by two amino acid changes that have not been previously described as important for *Arabidopsis* receptor function (Cao *et al.* 2014). However, 'Tango' mandarin is a much stronger responder to chitin than 'Washington navel' orange. In another study, Vetter *et al*. 2012 noted that the variation in FLS2 abundance for certain genotypes can reflect the variation in flg22 binding. We have also observed a segregation in response types among related species

– in response to the csp22 MAMP, some genotypes produce ROS but do not activate MAPK phosphorylation. This has been observed in *Arabidopsis* plants, where MAMPs that trigger receptor-like kinase pathways result in different immune outputs than those that trigger receptor-like protein pathways (Wan *et al.* 2018). There are multiple potential explanations for the segregation in the ability to perceive, the magnitude of perception, and differential immune outputs for related genotypes. Segregation of immune response types has been observed previously, where flg22 from *C*Las induces defense gene induction but no ROS burst in 'Sun Chu Sha Kat' mandarin (Shi *et al.* 2018). There is also a possibility that downstream signaling components may play a role in the magnitude of immune responses. Signaling has not been investigated in detail in perennial crops or outside of flg22 perception, and further research may reveal if downstream signaling components have a role in altering MAMP responsiveness in citrus.

Recent studies have identified immune receptor homologs that are capable of perceiving polymorphic flg22 epitopes that are not perceived by the canonical *Arabidopsis* FLS2 receptor. Flg22 from *Agrobacterium tumefaciens* contains several polymorphisms that prevent perception in *Arabidopsis* (Felix *et al.* 1999). Fürst *et al.* 2020 identified a novel flagellin-sensing receptor from wild grape with expanded ligand perception, $FLS2^{XL}$, capable of sensing both canonical flg22 and the *Agrobacterium* flg22 epitopes. The *Ralstonia solanacearum* flg22 is also highly polymorphic and is not recognized by tomato (Pfund *et al.* 2004). However, Wei *et al.* 2020 identified a FLS2/BAK1 complex in soybean that is capable of sensing the *Ralstonia* flg22. In this study, we have highlighted Rutaceae genotypes that are capable of recognizing canonical csp22 and $csp22_{CLas}$. In tomato, the CORE RLK is responsible for csp22 recognition (Wang *et al*. 2016). However, no obvious homolog of the CORE receptor has been identified in citrus genomes so far. There is likely an independently-evolved receptor that members of the Rutaceae possess to recognize csp22 epitopes. Comparative genomics of csp22-responsive and non-responsive citrus genotypes, or segregating populations if available, could be used to identify candidate receptor(s) for csp22 epitopes for future functional validation.

Flagellin perception is widespread amongst plants, mainly conferred by the receptor FLS2 (Saijo *et al.* 2018). FLS2 was first identified in *Arabidopsis thaliana* (Gómez-Gómez *et al.* 2000). The sequence of FLS2 from *Arabidopsis* was then used to identify and functionally characterize an FLS2 homolog in tomato (Robatzek *et al*. 2007). This strategy has been used to identify and characterize functional FLS2 homologs in a variety of plants, including grapevine (Trdá *et al*.

2013), citrus (Shi *et al*. 2016), and rice (Takai *et al.* 2008). From our study, LYK5 and CERK1 homologs are also widespread and cluster separately between dicots and monocots. Rice utilizes a different LysM receptor (CEBiP) along with the CERK1 co-receptor for chitin perception (Kaku *et al.* 2006, Lee *et al.* 2014, Shimizu *et al.* 2010). Cotton, a dicot, has a wall-associated kinase that interacts with LYK5 and CERK1 to promote chitin-induced dimerization (Wang *et al.* 2020). These results are consistent with an ancient acquisition of chitin perception in dicots, which may explain why a vast majority of the Rutaceae genotypes we evaluated are capable of producing an immune response to chitin. For MAMPs that can be recognized by a broad range of species, identifying receptors based on homology is still a useful tactic.

Our study highlights the diversity of immune response in a genetically diverse family of plants. We identified relatives of citrus that are capable of responding to a wide variety of MAMPs, opening up new opportunities to study relatives with potential novel mechanisms of immune signaling. The transfer of novel receptors for MAMPs to susceptible plants can generate resistance to pathogens (Hao *et al.* 2016, Fürst *et al.* 2020, Wei *et al.* 2020). ROS-based immune phenotyping can be a high-throughput method to accelerate selection of promising individuals in a breeding program. Individuals that can respond to unique MAMPs are likely to have unique immune signaling components that can be transferred to susceptible citrus varieties. A greater understanding of immune perception repertoires in economically important plant genotypes will also facilitate the design stacks of receptors for transfer and disease control. Similar strategies have resulted in durable resistance against fungal and oomycete pathogens in crop plants (Luo *et al.* 2021, Ghislain *et al.* 2018). This work has opened up interesting avenues to examine receptor diversity and identify new receptors in non-model species.

Materials and Methods

Plant materials and growth conditions

Eighty-six Rutaceae genotypes were tested for MAMP responsiveness under field and greenhouse conditions using mature trees (>5 years old). Field-grown trees in the Givaudan Citrus Variety Collection (GCVC) in Riverside, CA (http://www.citrusvariety.ucr.edu) were analyzed between the spring and fall from 2018-2021. Table **S1** includes all genotypes analyzed, their accession IDs, and their location. When collecting Rutaceae samples, branches

of selected Rutaceae genotypes were retrieved either from the greenhouse or the field, selecting branches with fully-expanded leaves that still retained flexibility. Branches were stored by placing the cut side of the branch into a wet floral block (Oasis® #10-00020-CASE) until processing.

Arabidopsis thaliana seeds (Col-0 or *lyk4/lyk5-2* mutant) were stratified for 2 days in the dark at 4°C before sowing onto soil or half-strength Murashige and Skoog (MS) media (Cao *et al.* 2014). Plants were grown in a Conviron growth chamber at 23°C and 70% relative humidity with a 10-h light/14-h dark photoperiod (100 μM m−2 s−1). 10- to 14-day-old seedlings grown on MS were used for MAPK phosphorylation and MTI marker gene induction assays, and four-week-old soil grown plants were used for ROS and MAPK assays.

Nicotiana benthamiana was grown in a growth chamber at 26°C with a 16-h light/8-h dark photoperiod (180 μM m−2 s−1). 30-day-old (before flowering) plants were used for *Agrobacterium*-mediated transient protein expression, and three- to 4-week-old plants were used to examine *LYK5* transgene expression.

Microbe-associated molecular patterns (MAMPs)

Immunogenic epitopes for flg22 and csp22 peptides were synthesized using Genscript (≥ 95% purity, Piscataway, NJ, USA). Hexaacetyl-chitohexaose (chitin) (Megazyme #O-CHI6) was diluted in water. The canonical flg22 epitope (QRLSTGSRINSAKDDAAGLQIA) is based on the sequence information from *Pseudomonas aeruginosa*. The canonical csp22 sequence (AVGTVKWFNAEKGFGFITPDGG) is from *Pseudomonas syringae*. The csp22 *C*Las sequence (HRGSIKWYNPDKGYGFITPEGS) is identical to the sequence from the *C*Las strain psy62 (CLIBASIA_04060).

Reactive oxygen species (ROS) burst assay

Leaf disks were collected using a #1 cork borer (4 mm) and floated overnight in 200 μL demineralized water in a Corning™ Costar™ 96-Well White Solid Plate (Fisher #07-200-589) with a plastic lid to prevent evaporation of the water. The subsequent day, water was replaced with 100 μL of an assay solution containing MAMP. The assay solution contained 20 μM L-012

(a luminol derivative from Wako Chemicals USA #120-04891), 10 mg mL−1 horseradish peroxidase (Sigma), and MAMP. Concentrations used for MAMP treatments were: 100 nM flg22, 10 μM chitin, 100 nM csp22, or 200 nM $csp22_{CLas}$. Luminescence was measured using a GloMax®-Multi+ Reader (Promega) or TriStar LB 941 plate reader (Berthold Technologies). Significance of differences between experimental groups was determined using ANOVA and Tukey's test, $\alpha = 0.05$. At least 8 leaf discs were used in each replication, and the experiments were repeated at least three times with similar results.

For each plate, an average maximum RLUs for each tested MAMP-genotype combination were calculated from the maximum RLU of the 8 leaf disks after subtraction by the average water RLU. Across all ROS plates, average maximum RLUs were calculated based on all plates ran for each MAMP-genotype and a heatmap was created from the accumulated ROS data via custom R scripts (Github repository: DanielleMStevens/Divergent_citrus_response_to_PAMPs) including the following R packages: ComplexHeatmap (v2.5.1, Gu *et al.* 2016), circlize (v0.4.8, Gu *et al.* 2014).

Mitogen-activated protein kinase (MAPK) induction assay

For MAPK induction assays in citrus, leaf disks were collected using a #6 cork borer (12 mm) from accessions grown in UC Davis or UC Riverside greenhouses and floated overnight in 1 mL deionized water in a 24-well tissue culture plate (VWR #10062-896) with a plastic lid to prevent evaporation of the water. The subsequent day, water was replaced with 500 μL of either water or water containing MAMP before pressure-infiltrating for 2 minutes at 30 mm Hg in a vacuum desiccator (SP Bel-Art #F42025-0000). Leaf disks were collected at 0, 10, and 20 minutes after vacuum infiltration, flash frozen in liquid nitrogen, and ground up with pestles attached to an electric grinder (Conos AC-18S electric torque screwdriver) before adding 200 μL extraction buffer and grinding until homogenous. Protein extraction buffer contained 50 mM HEPES (pH 7.5), 50 mM NaCl, 10 mM EDTA, 0.2% Triton X-100, Pierce™ Protease Inhibitor Mini Tablets, EDTA-free (Thermo #A32955), Pierce™ Phosphatase Inhibitor Mini Tablets (Thermo #A32957). Samples were centrifuged at 15,000 rpm for 10 minutes to pellet cell debris.

Protein concentrations were quantified with the Pierce 660 nm Protein Assay Reagent (Thermo #22660) with Ionic Detergent Compatibility Reagent (Thermo #22663). MAPKs were visualized by anti-p44/42 MPK immunoblotting (1:2000, Cell Signaling Technology #4370L) with goat

anti-rabbit HRP secondary antibody (1:3000, Bio-Rad #170-5046). Membranes were developed using the SuperSignal West Pico Chemiluminescent Substrate kit (Fisher #PI34578) and visualized on a ChemiDoc™ Touch Gel Imaging System (BioRad #1708370).

For MAPK induction assays in *Arabidopsis*, 5 day-old seedlings were transplanted into an 48-well tissue culture plate (Costar #3548) supplemented with half-strength MS liquid media. After 9 days, MS liquid media were replaced with 500 µL of either water or water containing 10 µM chitin. Three seedlings per treatment were collected at 0 and 15 minutes after chitin induction. Protein extraction and western blotting were conducted as described above.

qPCR

RNA was extracted from plant samples with TRIzol (Fisher #15596018), following the manufacturer's instructions. DNase treatments for RNA preps were performed with RQ1 RNase-Free DNase (Promega #PR-M6101). cDNA synthesis was performed with the MMLV Reverse Transcriptase (Promega #PRM1705) kit.

To examine the expression of *LYK5* homologs, citrus leaves were harvested to make leaf punches with a #9 cork borer (22.5 mm). Each leaf disk was placed in a 12-well plate (VWR #10062-894) with 1 mL water and kept overnight at room temperature to allow the samples to recover from wounding. The subsequent day, water was replaced with either 1 mL water or water containing 1 mL 10 µM chitin before vacuum-infiltrating for 1.5 minutes at 30 mm Hg in a vacuum desiccator (SP Bel-Art #F42025-0000). Three leaf disks per treatment were collected at 0 and 24 h post infiltration and RNA extraction was performed as described above.

A table of qPCR primers can be found in Table **S2**. Citrus *COX* (cytochrome oxidase subunit, Li *et al.* 2006) was used as the reference gene for qRT-PCR reactions. qPCR reactions were performed with SsoFast EvaGreen Supermix with Low ROX (BioRad #1725211) in a 96-well white PCR plate (BioRad #HSP9601) according to the manufacturer's instructions.
Fold-induction of gene expression determined using the $2^{-\Delta\Delta Ct}$ method (Livak and Schmittgen 2001), normalizing to water-treated and 0-hour timepoints.

Phylogenetic analyses and receptor comparisons

Plant genotypes used to build LYK5 and CERK1 phylogenies can be found in Table **S3** and **S4,** respectively. Using the *Arabidopsis thaliana* (NCBI taxid: 3702) CERK1$_{At}$ (NCBI RefSeq: NP_566689.2) and LYK5$_{At}$ (NCBI RefSeq: NP_180916.1) as queries, a blastp search was performed to mine for homologs across higher plant species (BLAST Suite v2.11.0+, query coverage cutoff 80%, E-value cutoff 1e-50, defaults otherwise). Partial protein hits were removed. Hits were then compared to all LysM RLKs in *A. thaliana* (CERK1, LYK2, LYK3, LYK4, and LYK5) and homologs closer to another LYK were removed. A multiple sequence alignment of receptor homologs was built using MAFFT (v7.310, --reorder, --maxiterate 1000, --localpair, defaults otherwise). TrimAl was used to trim each multiple sequence alignment for large gaps (v1.4.rev15, automated1, defaults otherwise). A maximum likelihood tree was built from the alignment using iqtree (v2.1.2, —bb 1000, -T AUTO, -st AA, -v -m MFP -safe, defaults otherwise), mid-rooted, and visualized using R packages phangorn (v2.7.1) and ggtree (v3.1.2.991).

We sought to characterize the number of chitin-binding LysM domains in LYK5 and CERK1 homologs. The standard domain prediction software Interproscan was unable to accurately predict even well characterized LYK5$_{At}$ and CERK1$_{At}$ receptors. To improve assessment of LysM domain frequency, we used homology and a hidden Markov model approach by blastp and HMMER, respectively. Hmmersearch using the LysM domain (query ID: PF01476.19) as a query identified the number of LysM domains (hmmer v3.1b2, -E 1e-5, defaults otherwise) (Eddy 2011). Manually extracted LysM domains from *A. thaliana* Col-0 were used to build a local blast database to calculate similarity of each LysM domain (coverage cutoff 80%, E-value cutoff 1e-50, defaults otherwise). All LysM domain analyses were plotted onto the receptor trees in R.

Ectodomains of all receptor homologs were extracted and an all-by-all comparison was computed using blastp. Similarity to either CERK1$_{At}$ and LYK5$_{At}$ or all citrus homologs to each other was plotted using R packages ggplot2 (v3.3.5) and ggbeeswarm (v0.6.0). Weblogos were generated from the multiple sequence alignment corresponding to LYK5$_{At}$ residues Y128 and S206 using WebLogo3 (Crooks *et al*. 2004).

The phylogenetic tree of citrus CORE homologs was built with CORE homologs from other solanaceous plants (Solanum_lycopersicum: Solyc03g096190; Solanum_pennellii: XP_015068909.1; Nicotiana_benthamiana: Niben101Scf02323g01010.1; Nicotiana_sylvestris: XP_009803840.1; Nicotiana_tabacum: XP_016470062.1). Protein sequences were aligned via

MAFFT, tree building was performed by iqtree, and were visualized in R similarly as described above. Sequences of cloned CORE homologs from 'Frost nucellar Eureka' lemon and 'Washington navel' orange are deposited in GenBank (ON863917 and ON863918, respectively).

For more information and raw files see Github repository: DanielleMStevens/Divergent_citrus_response_to_PAMPs.

Cloning citrus LYK5 homologous sequences and transcomplementation in Arabidopsis

Putative LYK5 sequences from Australian finger lime, 'Rio Red' grapefruit, 'Frost Lisbon' lemon, 'Tango' mandarin and Eremolemon were amplified using iProof DNA polymerase (Bio-Rad #BR0114). The PCR products were initially cloned into a pENTR™/D-TOPO™ backbone (Invitrogen #K2400-20), then LYK5 from 'Tango' mandarin (TM) was selected and inserted into a modified pGWB14 binary destination vector with the *Arabidopsis* ubiquitin 10 promoter using Gateway LR Clonase™ II enzyme mix (Invitrogen #11791-100). The *Arabidopsis lyk4/lyk5-2* mutant (Cao *et al.* 2014) was transformed using a floral dip method with pUBQ10::TM_LYK5-HA and pUBQ10::LYK5-HA from *Arabidopsis* (Zhang et al. 2006). Experiments were performed with T4 homozygous lines.

Transient expression in Nicotiana

The closest CORE homologs from 'Frost nucellar Eureka' lemon and 'Washington navel' orange were amplified using iProof DNA polymerase (Bio-Rad #BR0114). PCR products were cloned into a pEARLY103 backbone (Earley *et al.* 2006) with expression mediated by a 35S promoter, and plasmids were transformed via electroporation into *Agrobacterium* GV3101. *Nicotiana benthamiana* CORE was used as a positive control (Wang *et al.* 2016). To test the function of CORE homologs, young (non-flowering) *Nicotiana benthamiana* plants were infiltrated with *Agrobacterium* suspensions of OD_{600} 0.25. 24 hours after infiltration, leaf disks were collected using a #1 cork borer (4 mm) for ROS Assays as described above. To visualize the expression of CORE homologs, additional leaf disks were collected using a #7 cork borer at 48 hpi for protein extraction. Leaf disks were homogenized in 100 µL Laemmli buffer and boiled for 5 min.

Western blotting was conducted as described above and visualized with anti GFP-HRP antibody (Miltenyi Biotec #130-091-833).

Comparison of LYK5 *homologs in citrus*

Genome sequences surrounding *LYK5* homologs in 'Midknight Valencia' orange, 'Washington navel' orange and 'Tango' mandarin were compared based on BLASTp hits e-value 0.001 (Altschul, et al. 1990) against *de novo* assembled genomes. Contigs were assembled using wtgbt2 (Ruan and Li *et al.* 2020) and long-read sequencing was performed on the Pacific Biosciences Sequel II platform in the CLR sequencing mode. LYK5 protein sequences of 'Midknight Valencia' orange, 'Washington navel' orange and 'Tango' mandarin were aligned using MUSCLE v5.1 (Edgar 2021). The sequences of contigs and LYK5 protein of 'Washington navel' orange and 'Tango' mandarin are deposited in GenBank (*Citrus reticulata* ON685188, *Citrus sinensis* ON685189 and *Citrus reticulata* ON685190, *Citrus sinensis* ON685191).

Acknowledgements

We thank Dr. Melanie Schori (National Germplasm resources Laboratory Botanist, USDA-ARS) for help with the taxonomy of Rutaceae and the Citrus Research Board for their continued support (Project 5200-171 to DKS and 5200-157 to GC). We thank Mikeal Roose for funding the 'Tango' mandarin genome assembly and Georg Felix for providing a binary vector containing *Nicotiana CORE* and Erika Roxana Espinoza for assisting with ROS assays. Funding was provided by USDA-NIFA grant no. 2019-70016-29796 and NIH grant no. R35GM136402 awarded to GC. DMS was supported by the USDA-NIFA predoctoral fellowship grant no. 2021-67034-35049. TL was supported by the China Scholarship Council No. 201906300032.

Author Contributions

JF, TT, CR, and GC designed the research, and JT, TL, JF, TT, CR, RP, and JW performed the research. JT, TL, DMS, JF, TT, ST, CR and GC analyzed the data, and JT, TL, DMS, and GC wrote the paper.

DKS and EAD provided citrus sequencing data.

TLK provided guidance and access to greenhouse-grown Rutaceae genotypes.

Data Availability

The data that support the findings of this study are available, with raw data available from the corresponding author upon request. The sequences of contigs and LYK5 protein of 'Washington navel' orange and 'Tango' mandarin are deposited in GenBank (*Citrus reticulata* ON685188, *Citrus sinensis* ON685189 and *Citrus reticulata* ON685190, *Citrus sinensis* ON685191). Software used to build the heatmap and parts of Figure **4** are deposited in GitHub under the repository DanielleMStevens/Divergent_citrus_response_to_PAMPs. Sequences of cloned CORE homologs from 'Frost nucellar Eureka' lemon and 'Washington navel' orange in Supporting Information **5b** are deposited in GenBank (ON863917 and ON863918, respectively).

References

Altschul SF, Gish W, Miller W, Myers EW, Lipman DJ. **1990**. Basic local alignment search tool. *Journal of Molecular Biology* **215**: 403–410.

Alves MN, Lopes SA, Raiol-Junior LL, Wulff NA, Girardi EA, Ollitrault P, Peña L. **2021**. Resistance to '*Candidatus* Liberibacter asiaticus,' the Huanglongbing Associated Bacterium, in Sexually and/or Graft-Compatible *Citrus* Relatives. *Frontiers in Plant Science* **11**.

Antolín-Llovera M, Petutsching EK, Ried MK, Lipka V, Nürnberger T, Robatzek S, Parniske M. **2014**. Knowing your friends and foes – plant receptor-like kinases as initiators of symbiosis or defence. *New Phytologist* **204**: 791–802.

Appelhans MS, Bayly MJ, Heslewood MM, Groppo M, Verboom GA, Forster PI, Kallunki JA, Duretto MF. **2021**. A new subfamily classification of the *Citrus* family (Rutaceae) based on six nuclear and plastid markers. *TAXON* **70**: 1035–1061.

Asai T, Tena G, Plotnikova J, Willmann MR, Chiu W-L, Gomez-Gomez L, Boller T, Ausubel FM, Sheen J. **2002**. MAP kinase signalling cascade in Arabidopsis innate immunity. *Nature* **415**: 977–983.

Bigeard J, Colcombet J, Hirt H. **2015**. Signaling Mechanisms in Pattern-Triggered Immunity (PTI). *Molecular Plant* **8**: 521–539.

Bové JM. **2006**. HUANGLONGBING: A DESTRUCTIVE, NEWLY-EMERGING, CENTURY-OLD DISEASE OF CITRUS. *Journal of Plant Pathology* **88**: 7–37.

Cao Y, Liang Y, Tanaka K, Nguyen CT, Jedrzejczak RP, Joachimiak A, Stacey G. **2014**. The kinase LYK5 is a major chitin receptor in *Arabidopsis* and forms a chitin-induced complex with related kinase CERK1 (T Nürnberger, Ed.). *eLife* **3**: e03766.

Caruso M, Smith MW, Froelicher Y, Russo G, Gmitter FG. **2020**. Chapter 7 - Traditional breeding. In: Talon M, Caruso M, Gmitter FG, eds. The Genus Citrus. Woodhead Publishing, 129–148.

Castle WS. **2010**. A Career Perspective on Citrus Rootstocks, Their Development, and Commercialization. *HortScience* **45**: 11–15.

Chen Y, Bendix C, Lewis JD. **2019**. Comparative genomics screen identifies microbe-associated molecular patterns from *Candidatus* Liberibacter sp. that elicit immune responses in plants. *Mol. Plant. Microbe. Interact.*

Cheng JHT, Bredow M, Monaghan J, diCenzo GC. **2021**. Proteobacteria Contain Diverse flg22 Epitopes That Elicit Varying Immune Responses in *Arabidopsis thaliana*. *Molecular Plant-Microbe Interactions®* **34**: 504–510.

Cifuentes-Arenas JC, Beattie GAC, Peña L, Lopes SA. **2019**. *Murraya paniculata* and *Swinglea glutinosa* as Short-Term Transient Hosts of '*Candidatus* Liberibacter asiaticus' and Implications for the Spread of Huanglongbing. *Phytopathology®* **109**: 2064–2073.

Coletta-Filho HD, Castillo AI, Laranjeira FF, de Andrade EC, Silva NT, de Souza AA, Bossi ME, Almeida RPP, Lopes JRS. **2020**. Citrus Variegated Chlorosis: an Overview of 30 Years of Research and Disease Management. *Tropical Plant Pathology* **45**: 175–191.

Couto D, Zipfel C. **2016**. Regulation of pattern recognition receptor signalling in plants. *Nature Reviews Immunology* **16**: 537–552.

Crooks GE, Hon G, Chandonia J-M, Brenner SE. **2004**. WebLogo: A Sequence Logo Generator. *Genome Research* **14**: 1188–1190.

Dalio RJD, Magalhães DM, Rodrigues CM, Arena GD, Oliveira TS, Souza-Neto RR, Picchi SC, Martins PMM, Santos PJC, Maximo HJ, *et al.* 2017. PAMPs, PRRs, effectors and R-genes associated with citrus–pathogen interactions. *Annals of Botany* **119**: 749–774.

Das AK. **2003**. Citrus canker-A review. *Journal of Applied Horticulture* **5**: 52–60.

Earley KW, Haag JR, Pontes O, Opper K, Juehne T, Song K, Pikaard CS. **2006**. Gateway-compatible vectors for plant functional genomics and proteomics. *The Plant Journal* **45**: 616–629.

Eddy SR. **2011**. Accelerated Profile HMM Searches. *PLOS Computational Biology* **7**: e1002195.

Edgar RC. **2021**. MUSCLE v5 enables improved estimates of phylogenetic tree confidence by ensemble bootstrapping. : 2021.06.20.449169.

Erwig J, Ghareeb H, Kopischke M, Hacke R, Matei A, Petutschnig E, Lipka V. **2017**. Chitin-induced and CHITIN ELICITOR RECEPTOR KINASE1 (CERK1) phosphorylation-dependent endocytosis of *Arabidopsis thaliana* LYSIN MOTIF-CONTAINING RECEPTOR-LIKE KINASE5 (LYK5). *New Phytologist* **215**: 382–396.

Ference CM, Gochez AM, Behlau F, Wang N, Graham JH, Jones JB. **2018**. Recent advances in the understanding of *Xanthomonas citri* ssp. *citri* pathogenesis and citrus canker disease management. *Molecular Plant Pathology* **19**: 1302–1318.

Fürst U, Zeng Y, Albert M, Witte AK, Fliegmann J, Felix G. **2020**. Perception of *Agrobacterium tumefaciens* flagellin by FLS2XL confers resistance to crown gall disease. *Nature Plants* **6**: 22–27.

Gmitter FG, Hu X. **1990**. The possible role of Yunnan, China, in the origin of contemporary citrus species (rutaceae). *Economic Botany* **44**: 267–277.

Gómez-Gómez L, Boller T. **2000**. FLS2: An LRR Receptor–like Kinase Involved in the Perception of the Bacterial Elicitor Flagellin in *Arabidopsis*. *Molecular Cell* **5**: 1003–1011.

Gu Z, Eils R, Schlesner M. **2016**. Complex heatmaps reveal patterns and correlations in multidimensional genomic data. *Bioinformatics* **32**: 2847–2849.

Gu Z, Gu L, Eils R, Schlesner M, Brors B. **2014**. circlize implements and enhances circular visualization in R. *Bioinformatics* **30**: 2811–2812.

Hodges AW, Spreen TH. Economic Impacts of Citrus Greening (HLB) in Florida,. : 6.

Jaouad M, Moinina A, Ezrari S, Lahlali R. **2020**. Key pests and diseases of citrus trees with emphasis on root rot diseases: An overview. *Moroccan Journal of Agricultural Sciences* **1**.

Kaku H, Nishizawa Y, Ishii-Minami N, Akimoto-Tomiyama C, Dohmae N, Takio K, Minami E, Shibuya N. **2006**. Plant cells recognize chitin fragments for defense signaling through a plasma membrane receptor. *Proceedings of the National Academy of Sciences* **103**: 11086–11091.

Kamatyanatti M, Singh S, Sekhon B. **2021**. MUTATION BREEDING IN CITRUS- A REVIEW. *Plant Cell Biotechnology and Molecular Biology* **22**: 1–8.

Kubitzki K, Kallunki JA, Duretto M, Wilson PG. **2011**. Rutaceae. In: Kubitzki K, ed. The Families and Genera of Vascular Plants. Flowering Plants. Eudicots: Sapindales, Cucurbitales, Myrtaceae. Berlin, Heidelberg: Springer, 276–356.

Latado RR, Neto AT, Figueira A. In Vivo and in Vitro Mutation Breeding of Citrus.

Lee W-S, Rudd JJ, Hammond-Kosack KE, Kanyuka K. **2014**. *Mycosphaerella graminicola* LysM Effector-Mediated Stealth Pathogenesis Subverts Recognition Through Both CERK1 and CEBiP Homologues in Wheat. *Molecular Plant-Microbe Interactions®* **27**: 236–243.

Li W, Hartung JS, Levy L. **2006**. Quantitative real-time PCR for detection and identification of *Candidatus* Liberibacter species associated with citrus huanglongbing. *Journal of Microbiological Methods* **66**: 104–115.

Liao D, Sun X, Wang N, Song F, Liang Y. **2018**. Tomato LysM Receptor-Like Kinase SlLYK12 Is Involved in Arbuscular Mycorrhizal Symbiosis. *Frontiers in Plant Science* **9**.

Liu Y, Heying E, Tanumihardjo SA. **2012**. History, Global Distribution, and Nutritional Importance of Citrus Fruits. *Comprehensive Reviews in Food Science and Food Safety* **11**: 530–545.

Livak KJ, Schmittgen TD. **2001**. Analysis of relative gene expression data using real-time quantitative PCR and the 2(-Delta Delta C(T)) Method. *Methods* **25**: 402–408.

Magalhães DM, Scholte LLS, Silva NV, Oliveira GC, Zipfel C, Takita MA, De Souza AA. **2016**. LRR-RLK family from two *Citrus* species: genome-wide identification and evolutionary aspects. *BMC Genomics* **17**: 623.

Meng X, Zhang S. **2013**. MAPK Cascades in Plant Disease Resistance Signaling. *Annual Review of Phytopathology* **51**: 245–266.

Miya A, Albert P, Shinya T, Desaki Y, Ichimura K, Shirasu K, Narusaka Y, Kawakami N, Kaku H, Shibuya N. **2007**. CERK1, a LysM receptor kinase, is essential for chitin elicitor signaling in *Arabidopsis*. *Proceedings of the National Academy of Sciences* **104**: 19613–19618.

Miyata K, Kozaki T, Kouzai Y, Ozawa K, Ishii K, Asamizu E, Okabe Y, Umehara Y, Miyamoto A, Kobae Y, *et al.* 2014. The Bifunctional Plant Receptor, OsCERK1, Regulates Both Chitin-Triggered Immunity and Arbuscular Mycorrhizal Symbiosis in Rice. *Plant and Cell Physiology* **55**: 1864–1872.

Morton CM. **2009**. Phylogenetic relationships of the Aurantioideae (Rutaceae) based on the nuclear ribosomal DNA ITS region and three noncoding chloroplast DNA regions, atpB-rbcL spacer, rps16, and trnL-trnF. *Organisms Diversity & Evolution* **9**: 52–68.

Nagano Y, Mimura T, Kotoda N, Matsumoto R, Nagano AJ, Honjo MN, Kudoh H, Yamamoto M. **2018**. Phylogenetic relationships of Aurantioideae (Rutaceae) based on RAD-Seq. *Tree Genetics & Genomes* **14**: 6.

Newman M-A, Sundelin T, Nielsen J, Erbs G. **2013**. MAMP (microbe-associated molecular pattern) triggered immunity in plants. *Frontiers in Plant Science* **4**.

Ngou BPM, Ding P, Jones JDG. **2022**. Thirty years of resistance: Zig-zag through the plant immune system. *The Plant Cell*: koac041.

Pfund C, Tans-Kersten J, Dunning FM, Alonso JM, Ecker JR, Allen C, Bent AF. **2004**. Flagellin Is Not a Major Defense Elicitor in *Ralstonia solanacearum* Cells or Extracts Applied to *Arabidopsis thaliana*. *Molecular Plant-Microbe Interactions®* **17**: 696–706.

Ramadugu C, Keremane ML, Halbert SE, Duan YP, Roose ML, Stover E, Lee RF. **2016**. Long-Term Field Evaluation Reveals Huanglongbing Resistance in *Citrus* Relatives. *Plant Disease* **100**: 1858–1869.

Reece PC, Swingle WT. **1967**. The botany of Citrus and its wild relatives. *The citrus industry* **1**: 190–430.

Robatzek S, Bittel P, Chinchilla D, Köchner P, Felix G, Shiu S-H, Boller T. **2007**. Molecular identification and characterization of the tomato flagellin receptor LeFLS2, an orthologue of *Arabidopsis* FLS2 exhibiting characteristically different perception specificities. *Plant Molecular Biology* **64**: 539–547.

Roberts R, Mainiero S, Powell AF, Liu AE, Shi K, Hind SR, Strickler SR, Collmer A, Martin GB. **2019**. Natural variation for unusual host responses and flagellin-mediated immunity against *Pseudomonas syringae* in genetically diverse tomato accessions. *New Phytologist* **223**: 447–461.

Ruan J, Li H. **2020**. Fast and accurate long-read assembly with wtdbg2. *Nature Methods* **17**: 155–158.

Saijo Y, Loo EP, Yasuda S. **2018**. Pattern recognition receptors and signaling in plant–microbe interactions. *The Plant Journal* **93**: 592–613.

Shi Q, Febres VJ, Jones JB, Moore GA. **2015**. Responsiveness of different citrus genotypes to the *Xanthomonas citri* ssp. *citri*-derived pathogen-associated molecular pattern (PAMP) flg22 correlates with resistance to citrus canker. *Molecular Plant Pathology* **16**: 507–520.

Shi Q, Febres VJ, Jones JB, Moore GA. **2016**. A survey of FLS2 genes from multiple citrus species identifies candidates for enhancing disease resistance to *Xanthomonas citri* ssp. *citri*. *Horticulture Research* **3**: 16022.

Shi Q, Febres VJ, Zhang S, Yu F, McCollum G, Hall DG, Moore GA, Stover E. **2018**. Identification of Gene Candidates Associated with Huanglongbing Tolerance, Using '*Candidatus* Liberibacter asiaticus' Flagellin 22 as a Proxy to Challenge Citrus. *Molecular Plant-Microbe Interactions*® **31**: 200–211.

Shimizu T, Nakano T, Takamizawa D, Desaki Y, Ishii-Minami N, Nishizawa Y, Minami E, Okada K, Yamane H, Kaku H, *et al.* 2010. Two LysM receptor molecules, CEBiP and OsCERK1, cooperatively regulate chitin elicitor signaling in rice. *The Plant Journal* **64**: 204–214.

Stover E, McCollum G, Ramos J, Jr RGS. **2014**. Growth, Health and Liberibacter asiaticus Titer in Diverse Citrus Scions on Mandarin versus Trifoliate Hybrid Rootstocks in a Field Planting with Severe Huanglongbing. *Proceedings of the Florida State Horticultural Society* **127**: 53–59.

Takai R, Isogai A, Takayama S, Che F-S. **2008**. Analysis of Flagellin Perception Mediated by flg22 Receptor OsFLS2 in Rice. *Molecular Plant-Microbe Interactions*® **21**: 1635–1642.

Trdá L, Fernandez O, Boutrot F, Héloir M-C, Kelloniemi J, Daire X, Adrian M, Clément C, Zipfel C, Dorey S, *et al.* 2014. The grapevine flagellin receptor VvFLS2 differentially recognizes flagellin-derived epitopes from the endophytic growth-promoting bacterium *Burkholderia phytofirmans* and plant pathogenic bacteria. *New Phytologist* **201**: 1371–1384.

USDA, National Agricultural Statistics Service. 2020. Citrus Fruits: 2020 Summary.

Uzun A, Yesiloglu T. **2012**. *Genetic Diversity in Citrus*. InTech.

Veluchamy S, Hind SR, Dunham DM, Martin GB, Panthee DR. **2014**. Natural Variation for Responsiveness to flg22, flgII-28, and csp22 and *Pseudomonas syringae* pv. *tomato* in Heirloom Tomatoes. *PLOS ONE* **9**: e106119.

Vetter MM, Kronholm I, He F, Häweker H, Reymond M, Bergelson J, Robatzek S, de Meaux J. **2012**. Flagellin Perception Varies Quantitatively in *Arabidopsis thaliana* and Its Relatives. *Molecular Biology and Evolution* **29**: 1655–1667.

Wan W-L, Zhang L, Pruitt R, Zaidem M, Brugman R, Ma X, Krol E, Perraki A, Kilian J, Grossmann G, *et al.* 2019. Comparing *Arabidopsis* receptor kinase and receptor protein-mediated immune signaling reveals BIK1-dependent differences. *The New Phytologist* **221**: 2080–2095.

Wang N. **2019**. The Citrus Huanglongbing Crisis and Potential Solutions. *Molecular Plant* **12**: 607–609.

Wang L, Albert M, Einig E, Fürst U, Krust D, Felix G. **2016**. The pattern-recognition receptor CORE of Solanaceae detects bacterial cold-shock protein. *Nature Plants* **2**: 1–9.

Wang X, Xu Y, Zhang S, Cao L, Huang Y, Cheng J, Wu G, Tian S, Chen C, Liu Y, *et al.* 2017. Genomic analyses of primitive, wild and cultivated citrus provide insights into asexual reproduction. *Nature Genetics* **49**: 765–772.

Wang P, Zhou L, Jamieson P, Zhang L, Zhao Z, Babilonia K, Shao W, Wu L, Mustafa R, Amin I, *et al.* 2020. The Cotton Wall-Associated Kinase GhWAK7A Mediates Responses to Fungal Wilt Pathogens by Complexing with the Chitin Sensory Receptors. *The Plant Cell* **32**: 3978–4001.

Wei Y, Balaceanu A, Rufian JS, Segonzac C, Zhao A, Morcillo RJL, Macho AP. **2020**. An immune receptor complex evolved in soybean to perceive a polymorphic bacterial flagellin. *Nature Communications* **11**: 3763.

Wu GA, Terol J, Ibanez V, López-García A, Pérez-Román E, Borredá C, Domingo C, Tadeo FR, Carbonell-Caballero J, Alonso R, *et al.* 2018. Genomics of the origin and evolution of *Citrus*. *Nature* **554**: 311–316.

Xue D-X, Li C-L, Xie Z-P, Staehelin C. **2019**. LYK4 is a component of a tripartite chitin receptor complex in *Arabidopsis thaliana*. *Journal of Experimental Botany* **70**: 5507–5516.

Yu Y, Chen C, Huang M, Yu Q, Du D, Mattia MR, Gmitter FG. **2018**. Genetic Diversity and Population Structure Analysis of Citrus Germplasm with Single Nucleotide Polymorphism Markers. *Journal of the American Society for Horticultural Science* **143**: 399–408.

Zhang W, Fraiture M, Kolb D, Löffelhardt B, Desaki Y, Boutrot FFG, Tör M, Zipfel C, Gust AA, Brunner F. **2013**. *Arabidopsis* RECEPTOR-LIKE PROTEIN30 and Receptor-Like Kinase SUPPRESSOR OF BIR1-1/EVERSHED Mediate Innate Immunity to Necrotrophic Fungi. *The Plant Cell* **25**: 4227–4241.

Zhang X, Henriques R, Lin S-S, Niu Q-W, Chua N-H. **2006**. *Agrobacterium*-mediated transformation of *Arabidopsis thaliana* using the floral dip method. *Nature Protocols* **1**: 641–646.

Zhong G, Nicolosi E. **2020**. Citrus Origin, Diffusion, and Economic Importance. In: Gentile A, La Malfa S, Deng Z, eds. Compendium of Plant Genomes. The Citrus Genome. Cham: Springer International Publishing, 5–21.

Figure legends

Figure 1. Genotypes within the Rutaceae family, including citrus, exhibit diverse responses to common MAMPs and possess differing leaf morphologies. A. Heat map compiling average max relative light units (RLUs) from reactive oxygen species (ROS) assays in genotypes within the Rutaceae family, organized by MAMP and phylogenetic relationship. Max RLUs are averages of at least three independent experiments and are represented as a heatmap, where *max RLU = (max RLU MAMP – max RLU water)*. <90 RLU is the threshold for no response. Asterisks indicate genotypes that exhibit a variable response, where one or two independent experiments shared a response. The MAMPs used are canonical features in the following concentrations: chitin (10 μM), flg22 (100 nM), csp22 (100 nM). B. Leaf, branch, and fruit morphologies of selected genotypes grown under greenhouse and field conditions. Scale bars = 2 cm. Genotypes are referred to by common name unless otherwise unavailable.

Figure 2. Rutaceae genotypes vary in the magnitude of their responses to perception of chitin, flagellin and cold shock protein immunogenic epitopes. A. Distribution of all average max RLU values, with gray lines indicating 25th and 75th percentile markings. Box plots below are organized by the magnitude of their responses to chitin (B), flg22 (C), and csp22 (D). The MAMPs used are canonical features in the following concentrations: chitin (10 μM), flg22 (100 nM), csp22 (100 nM). Max RLUs are averages of at least three independent experiments, where *max RLU = (max RLU MAMP – max RLU water)*. Data points on box plots represent the average max RLU for an individual experiment, with n = 8 leaf disks per experiment. Criteria for the response categories: “strong” responders are in the top 25th percentile, “medium” responders are between the 25th and 75th percentiles, and “weak” responders are in the bottom 25th percentile. The bar within the box plot depicts the median of the data, where the box boundaries represent the interquartile range (between the 25th and 75th percentiles) of the

data. Box whiskers represent the minimum or maximum values of the data within 1.5x of the interquartile range.

Figure 3. ROS and MAPK induction in response to MAMP treatment in cultivated citrus and wild relatives. A. Box plots showing the average max RLUs of selected Rutaceae genotypes in response to chitin, flg22, and csp22. The MAMPs used are canonical features in the following concentrations: chitin (10 μM), flg22 (100 nM), csp22 (100 nM). Max RLUs are averages of at least three independent experiments, where *max RLU = (max RLU PAMP – max RLU water)*. Data points on box plots represent the average max RLU for an individual experiment, with n = 8 leaf disks per experiment. The bar within the box plot depicts the median of the data, where the box boundaries represent the interquartile range (between the 25th and 75th percentiles) of the data. Box whiskers represent the minimum or maximum values of the data within 1.5x of the interquartile range. B. MAPK induction visualized at 0, 10, and 20 min post-induction with water or MAMP. MAMPs are applied to leaf punches at the following concentrations for MAPK assays: chitin (10 μM), flg22 (100 nM), csp22 (100 nM), with water as a negative control. Western blots are performed with an anti-p42/44 MAPK antibody to visualize the MAPK bands and Coomassie Brilliant Blue (CBB) to verify equal loading of protein samples. All experiments were performed at least 3X with similar results.

Figure 4. Phylogeny of LYK5 and CERK1 receptor homologs. A. Maximum likelihood phylogenetic tree of 102 LYK5 and LYK5-like homologs (top) and 120 CERK1 and CERK1-like homologs (bottom) from 66 plant species. In both trees, eudicots are labeled in purple, monocots are labeled in green, and sequences from citrus varieties are labeled in red. 1000 ultrafast bootstrap replicates were calculated and values over 90 were plotted as a gray dot. To determine the number of LysM domains, hmmer (LysM domain, query ID: PF01476.19) and blastp was used. Similarity to the *Arabidopsis thaliana* LysM domains by blastp from LYK5 and CERK1 were calculated and plotted. Scale bar indicates tree distance. B. All-by-all blastp of LysM receptor ectodomains. Top: blastp comparison of LYK5 and CERK1 homologs from the Citrinae tribe. Bottom: blastp comparison of all LYK5 and CERK1 plant homologs using Arabidopsis as a query. C. Weblogos across 102 plant LYK5 homologs corresponding to critical residues for chitin binding in *A. thaliana* $LYK5_{At}$ Y128 and S206.

Figure 5. 'Washington navel' orange and 'Tango' mandarin have nearly identical LYK5 homologs, but differ in magnitude of their chitin response. A. ROS curve for 'Washington

navel' orange and 'Tango' mandarin (left) and 'Washington navel' orange only (right) when induced with either water or 10 μM chitin. Note the different scale on the y-axes. B. MAPK induction in response to either water for chitin in 'Washington navel' orange vs. 'Tango' mandarin using anti-p42/44 MAPK immunoblotting. Experiments were repeated 4 times. CBB = Coomassie Brilliant Blue. C. Genome organization of LYK5 in 'Midknight Valencia' orange, 'Washington navel' orange, and 'Tango' mandarin, with the LYK5 domain in 'Tango' mandarin expanded to show functional domains. Arrows indicate the difference in amino acid sequence between 'Tango' mandarin and 'Washington navel' orange. D. Normalized expression of the citrus $LYK5_{At}$ homolog measured via qPCR 24 h after water and chitin induction, using citrus COX as a reference gene. Error bars are standard deviation (n = 6 for water treatments, 9 for chitin treatments). WN = 'Washington navel' orange; TM = 'Tango' mandarin.

Figure 6. The 'Tango' mandarin $LYK5_{At}$ homolog can complement an *Arabidopsis* chitin perception mutant. A. ROS production of Arabidopsis *lyk4/lyk5-2* knockouts complemented with the indicated LYK5 constructs after treatment with 10 μM chitin. The bar within the box plot depicts the median of the data, where the box boundaries represent the interquartile range (between the 25th and 75th percentiles) of the data. Box whiskers represent the minimum or maximum values of the data within 1.5x of the interquartile range. Anti-HA-HRP immunoblots visualize the LYK5-HA bands; CBB = Coomassie Brilliant Blue (CBB). Significance of results was determined via ordinary one-way ANOVA, with a post hoc Dunnett's multiple comparison to the lyk4/lyk5-2 knockout. Asterisks represent significance thresholds: **** = p<0.0001, *** = p=0.0001 to 0.001, ** p=0.001 to 0.01, * p=0.01 to 0.05. B. MAPK induction in response to either water for chitin in LYK5-complemented Arabidopsis *lyk4/lyk5-2*, using anti-p42/44 MAPK immunoblotting. CBB = Coomassie Brilliant Blue. All experiments were performed 3 times with similar results.

Figure 7. Three Rutaceae subtribes can respond to a polymorphic csp22 from an important citrus pathogen. A. Alignment of the canonical csp22 sequence to the csp22 of *Candidatus* Liberibacter asiaticus ($csp22_{CLas}$). B. Heat map compiling average max relative light units (RLUs) from ROS assays in genotypes within the Rutaceae family, organized by MAMP and phylogenetic relationship. Max RLUs are averages of at least three independent experiments, where *max RLU = (max RLU PAMP – max RLU water)*. <90 RLU is the threshold for no response. Asterisks indicate genotypes that exhibit a variable response, where one or two independent experiments revealed a response. The MAMPs used for treatments are canonical

csp22 and csp22 from *Candidatus* Liberibacter asiaticus. C. Box plot of max RLUs for citrus relatives that can respond to 200 nM csp22$_{CLas}$. Max RLUs are averages of at least three independent experiments. Data points on box plots represent the average max RLU for an individual experiment, with n = 8 leaf disks per experiment. The max RLU are plotted on a log10 scale. The bar within the box plot depicts the median of the data, where the box boundaries represent the interquartile range (between the 25th and 75th percentiles) of the data. Box whiskers represent the minimum or maximum values of the data within 1.5x of the interquartile range. D. MAPK induction by csp22 or csp22$_{CLas}$ in either Valencia orange or *Clausena harmandiana*, visualized by p42/44 MAPK antibody immunoblotting. CBB = Coomassie Brilliant Blue.

Supporting Information

Supporting Information Table S1 contains information on the Rutaceae genotypes used for this study.

Supporting Information Table S2 contains information on primers used for this study.

Supporting Information Table S3 contains information on the LYK5 sequences used to build **Figure 4a.**

Supporting Information Table S4 contains information on the CERK1 sequences used to build **Figure 4a.**

Supporting Information Figure 1 contains representative ROS curves for selected weak, medium, and strong responders of MAMPs from **Figure 2**.

Supporting Information Figure 2 contains amino acid alignments of LYK5 homologs.

Supporting Information Figure 3 contains the full heat map of genotypes tested for **Figure 7**, including non-responders of either csp22 or csp22$_{CLas}$.

Supporting Information Figure 4 contains the visualization of MAMP perception in selected genotypes with HLB disease susceptibility from Ramadugu *et al.* 2016.

Supporting Information Figure 5 contains information on the closest citrus homologs of tomato CORE.

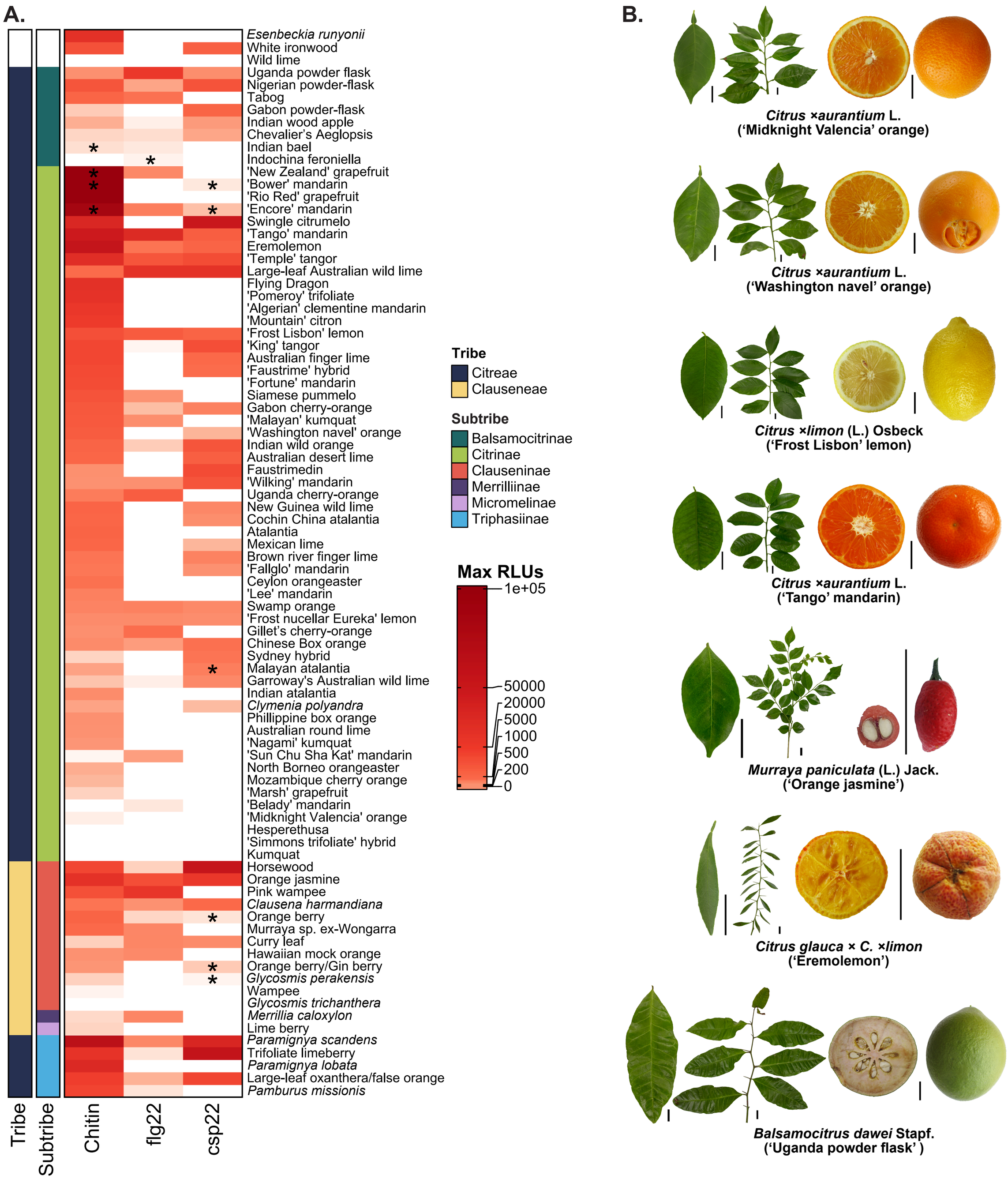

Figure 1. Genotypes within the Rutaceae family, including citrus, exhibit diverse responses to common MAMPs and possess differing leaf morphologies. A. Heat map compiling average max relative light units (RLUs) from reactive oxygen species (ROS) assays in genotypes within the Rutaceae family, organized by MAMP and phylogenetic relationship. White indicates genotypes in an unresolved tribe. Max RLUs are averages of at least three independent experiments and are represented as a heatmap, where *max RLU = (max RLU MAMP – max RLU water).* <90 RLU is the threshold for no response. Asterisks indicate genotypes that exhibit a variable response, where one or two independent experiments shared a response. The MAMPs used are canonical features in the following concentrations: chitin (10 μM), flg22 (100 nM), csp22 (100 nM). B. Leaf, branch, and fruit morphologies of selected genotypes grown under greenhouse and field conditions. Scale bars = 2 cm. Genotypes are referred to by common name unless otherwise unavailable.

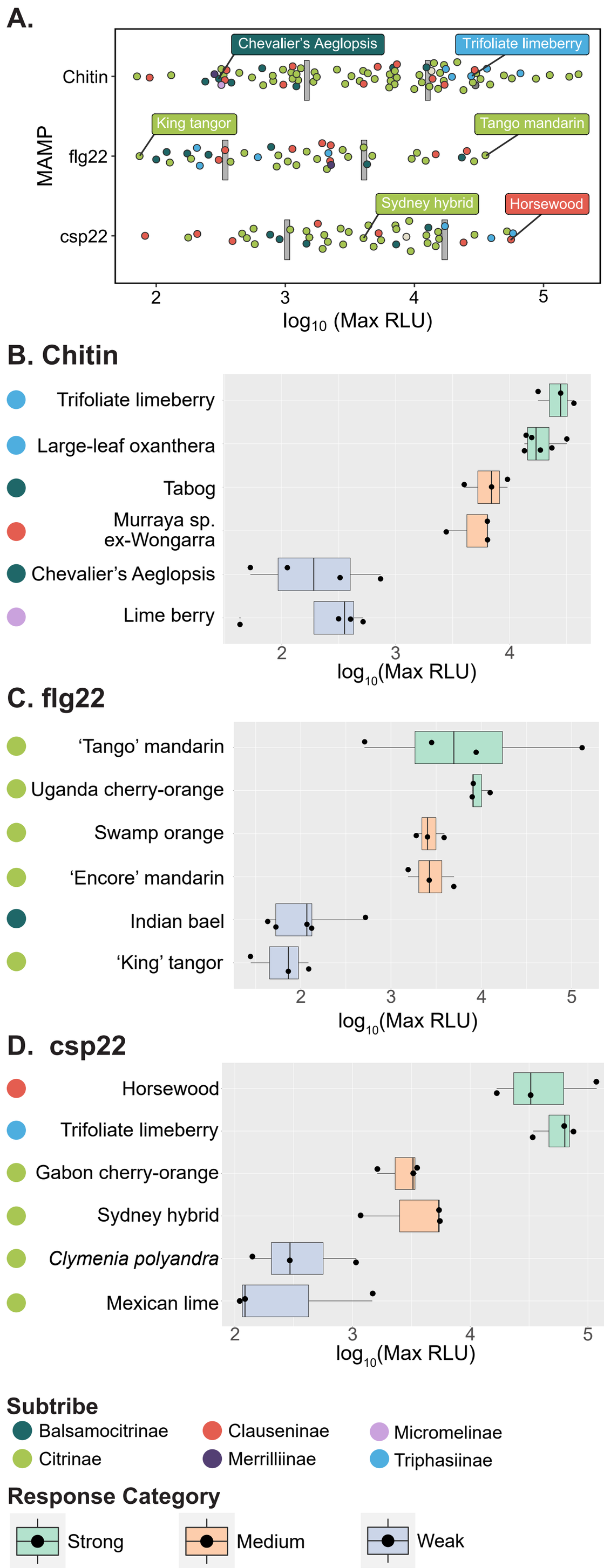

Figure 2. Rutaceae genotypes vary in the magnitude of their responses to perception of chitin, flagellin and cold shock protein immunogenic epitopes. A. Distribution of all average max RLU values, with gray lines indicating 25th and 75th percentile markings. Box plots below are organized by the magnitude of their responses to chitin (B), flg22 (C), and csp22 (D). The MAMPs used are canonical features in the following concentrations: chitin (10 µM), flg22 (100 nM), csp22 (100 nM). Max RLUs are averages of at least three independent experiments, where *max RLU = (max RLU MAMP – max RLU water)*. Data points on box plots represent the average max RLU for an individual experiment, with n = 8 leaf disks per experiment. Criteria for the response categories: "strong" responders are in the top 25th percentile, "medium" responders are between the 25th and 75th percentiles, and "weak" responders are in the bottom 25th percentile. The bar within the box plot depicts the median of the data, where the box boundaries represent the interquartile range (between the 25th and 75th percentiles) of the data. Box whiskers represent the minimum or maximum values of the data within 1.5x of the interquartile range.

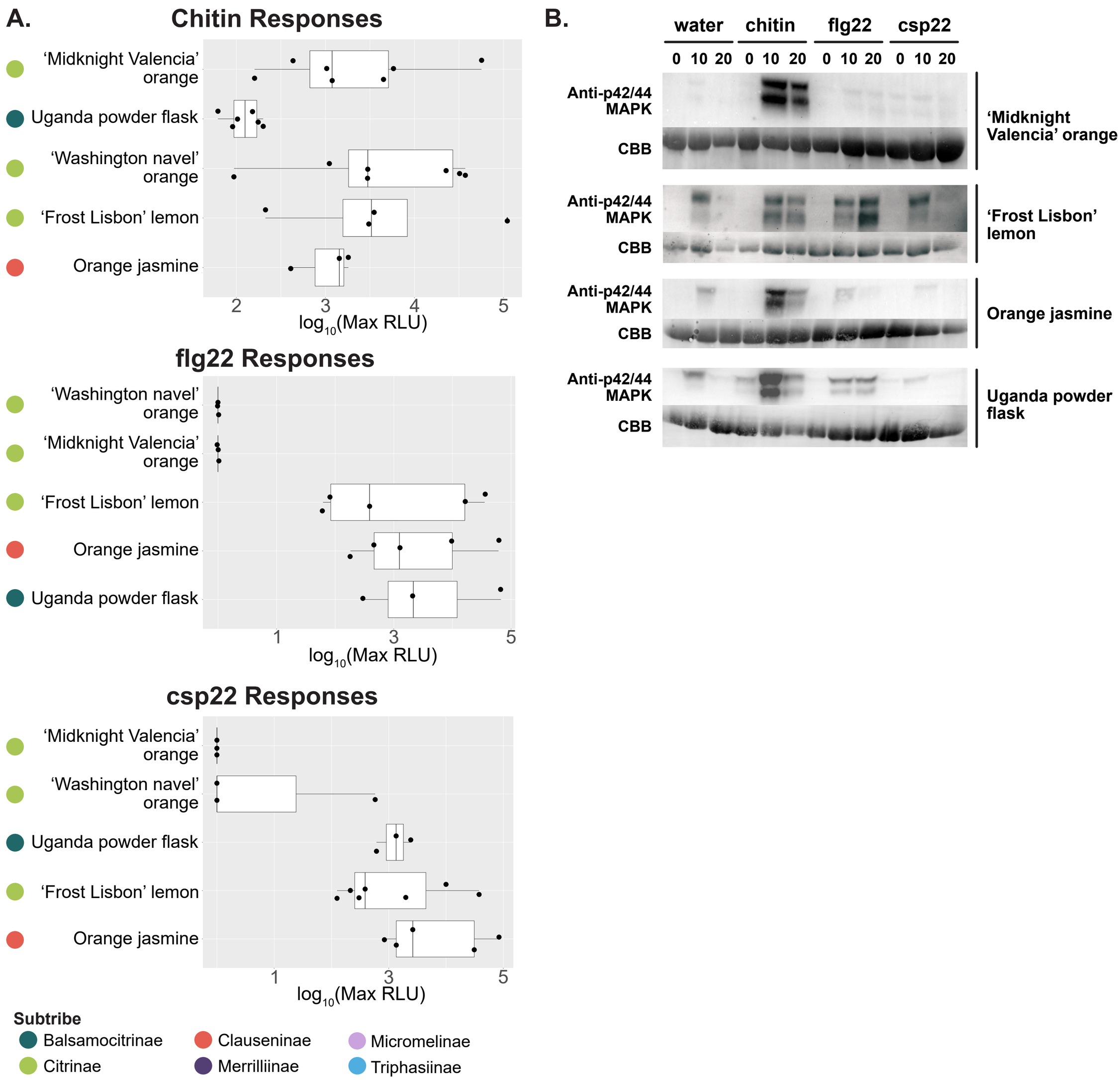

Figure 3. ROS and MAPK induction in response to MAMP treatment in cultivated citrus and wild relatives. A. Box plots showing the average max RLUs of selected Rutaceae genotypes in response to chitin, flg22, and csp22. The MAMPs used are canonical features in the following concentrations: chitin (10 μM), flg22 (100 nM), csp22 (100 nM). Max RLUs are averages of at least three independent experiments, where *max RLU = (max RLU PAMP – max RLU water)*. Data points on box plots represent the average max RLU for an individual experiment, with n = 8 leaf disks per experiment. The bar within the box plot depicts the median of the data, where the box boundaries represent the interquartile range (between the 25th and 75th percentiles) of the data. Box whiskers represent the minimum or maximum values of the data within 1.5x of the interquartile range. B. MAPK induction visualized at 0, 10, and 20 min post-induction with water or MAMP. MAMPs are applied to leaf punches at the following concentrations for MAPK assays: chitin (10 μM), flg22 (100 nM), csp22 (100 nM), with water as a negative control. Western blots are performed with an anti-p42/44 MAPK antibody to visualize the MAPK bands and Coomassie Brilliant Blue (CBB) to verify equal loading of protein samples. All experiments were performed at least 3X with similar results.

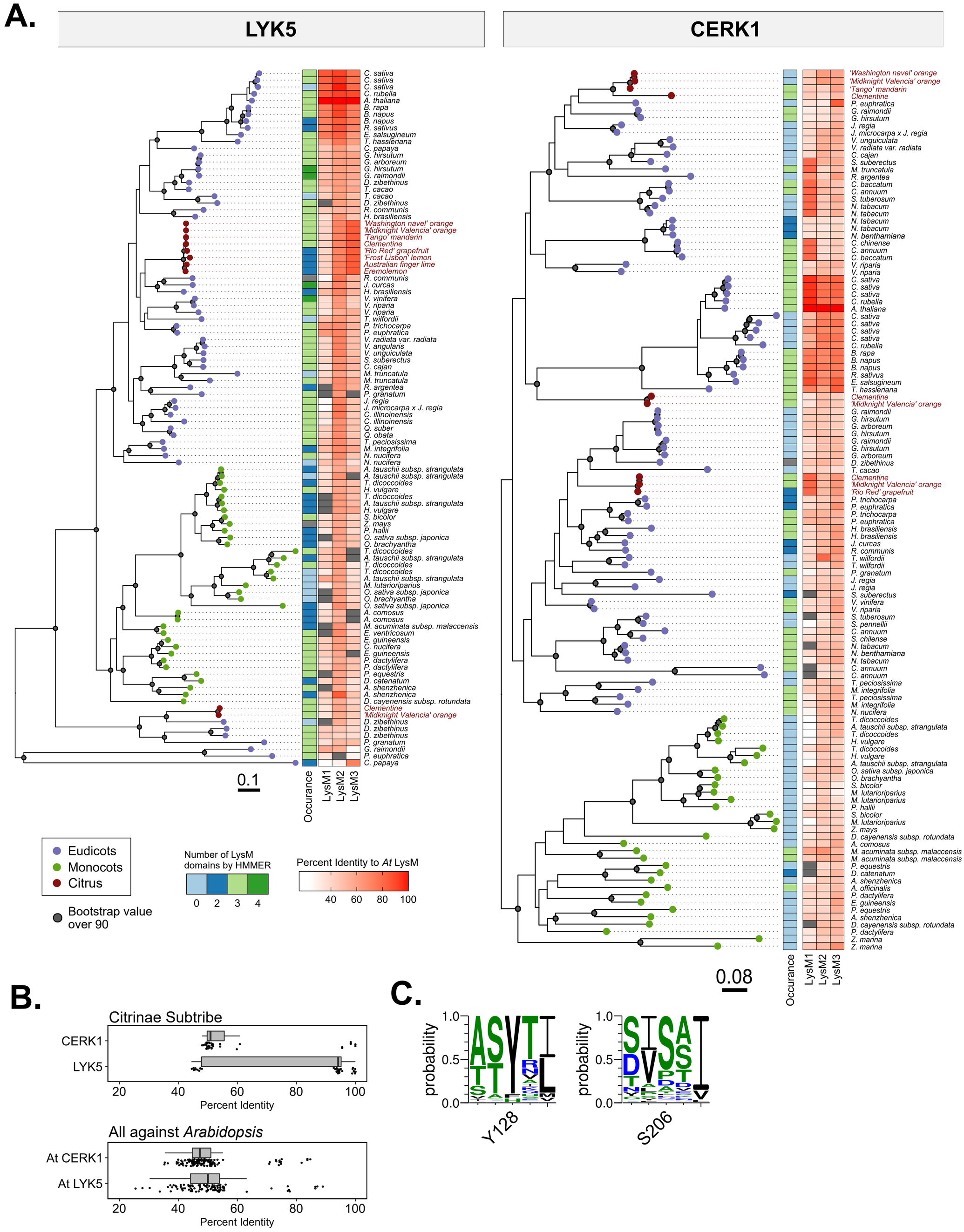

Figure 4. Phylogeny of LYK5 and CERK1 receptor homologs. A. Maximum likelihood phylogenetic tree of 101 LYK5 and LYK5-like homologs (top) and 120 CERK1 and CERK1-like homologs (bottom) from 66 plant species. In both trees, eudicots are labeled in purple, monocots are labeled in green, and sequences from citrus varieties are labeled in red. 1000 ultrafast bootstrap replicates were calculated and values over 90 were plotted as a gray dot. To determine the number of LysM domains, Hmmer (LysM domain, query ID: PF01476.19) and blastp was used. Similarity to the *Arabidopsis thaliana* LysM domains by blastp from LYK5 and CERK1 were calculated and plotted. Scale bar indicates tree distance. B. All-by-all blastp of LysM receptor ectodomains. Top: blastp comparison of LYK5 and CERK1 homologs from the Citrinae tribe. Bottom: blastp comparison of all LYK5 and CERK1 plant homologs using *Arabidopsis* as a query. C. Weblogos across 101 plant LYK5 homologs corresponding to critical residues for chitin binding in *A. thaliana* $LYK5_{At}$ Y128 and S206.

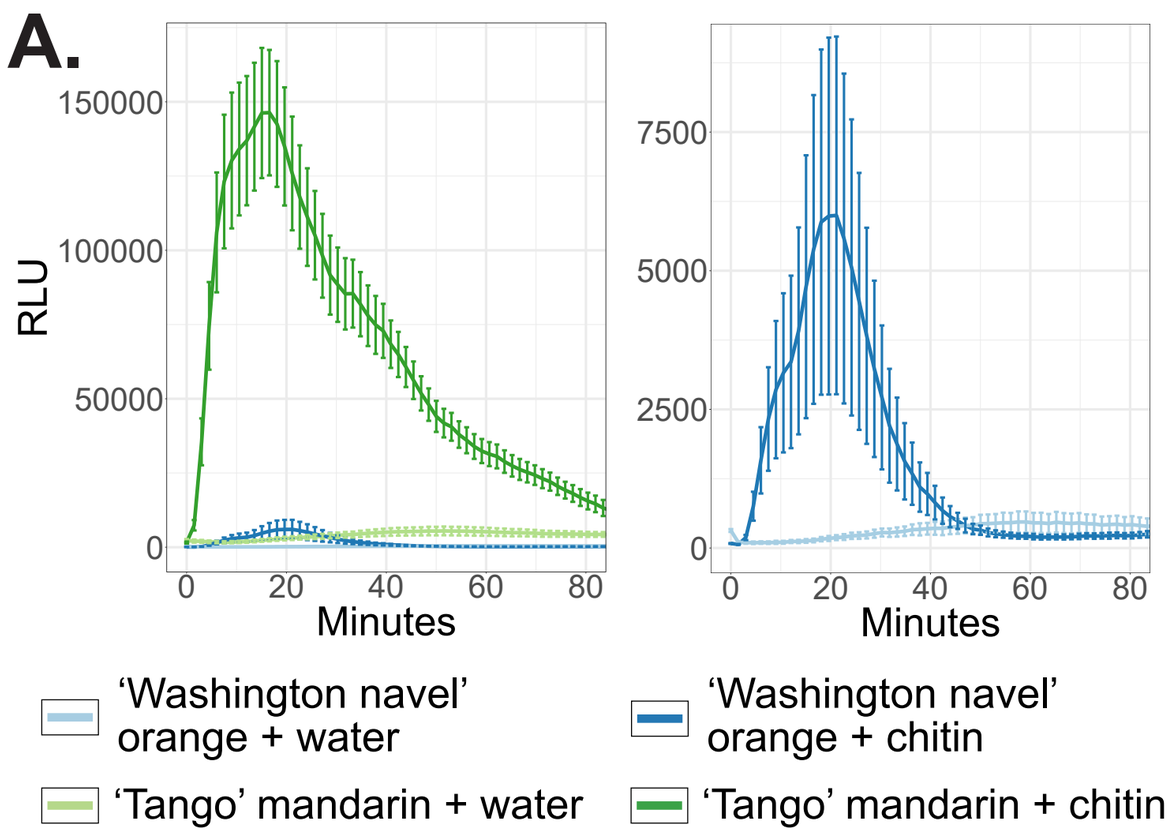

Figure 5. 'Washington navel' orange and 'Tango' mandarin have nearly identical LYK5 homologs, but differ in magnitude of their chitin response. A. ROS curve for 'Washington navel' orange and 'Tango' mandarin (left) and 'Washington navel' orange only (right) when induced with either water or 10 µM chitin. Note the different scale on the y-axes. B. MAPK induction in response to either water for chitin in 'Washington navel' orange vs. 'Tango' mandarin using anti-p42/44 MAPK immunoblotting. Experiments were repeated 4 times. CBB = Coomassie Brilliant Blue. C. Genome organization of LYK5 in 'Midknight Valencia' orange, 'Washington navel' orange, and 'Tango' mandarin, with the LYK5 domain in 'Tango' mandarin expanded to show functional domains. Arrows indicate the difference in amino acid sequence between 'Tango' mandarin and 'Washington navel' orange. D. Normalized expression of the citrus *LYK5*$_{At}$ homolog measured via qPCR 24 h after water and chitin induction, using citrus *COX* as a reference gene. Error bars are standard deviation (n = 6 for water treatments, 9 for chitin treatments). WN = 'Washington navel' orange; TM = 'Tango' mandarin.

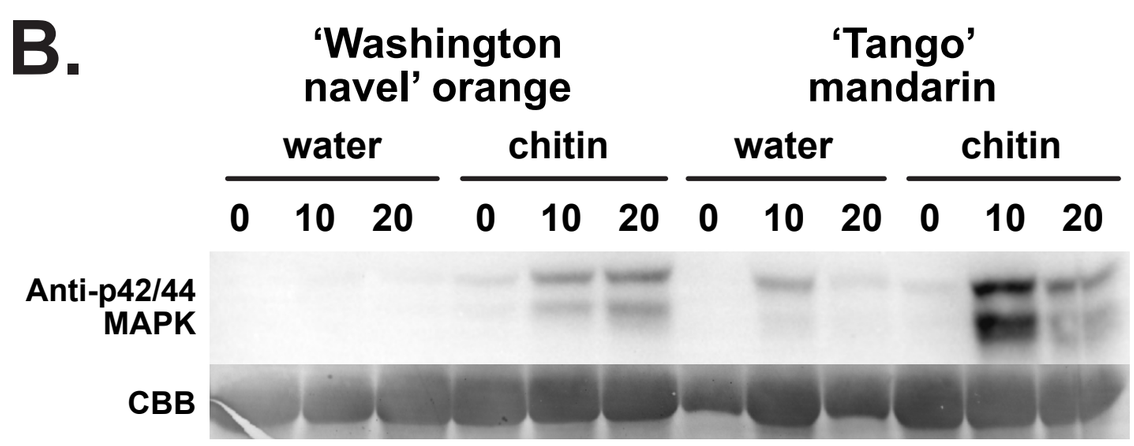

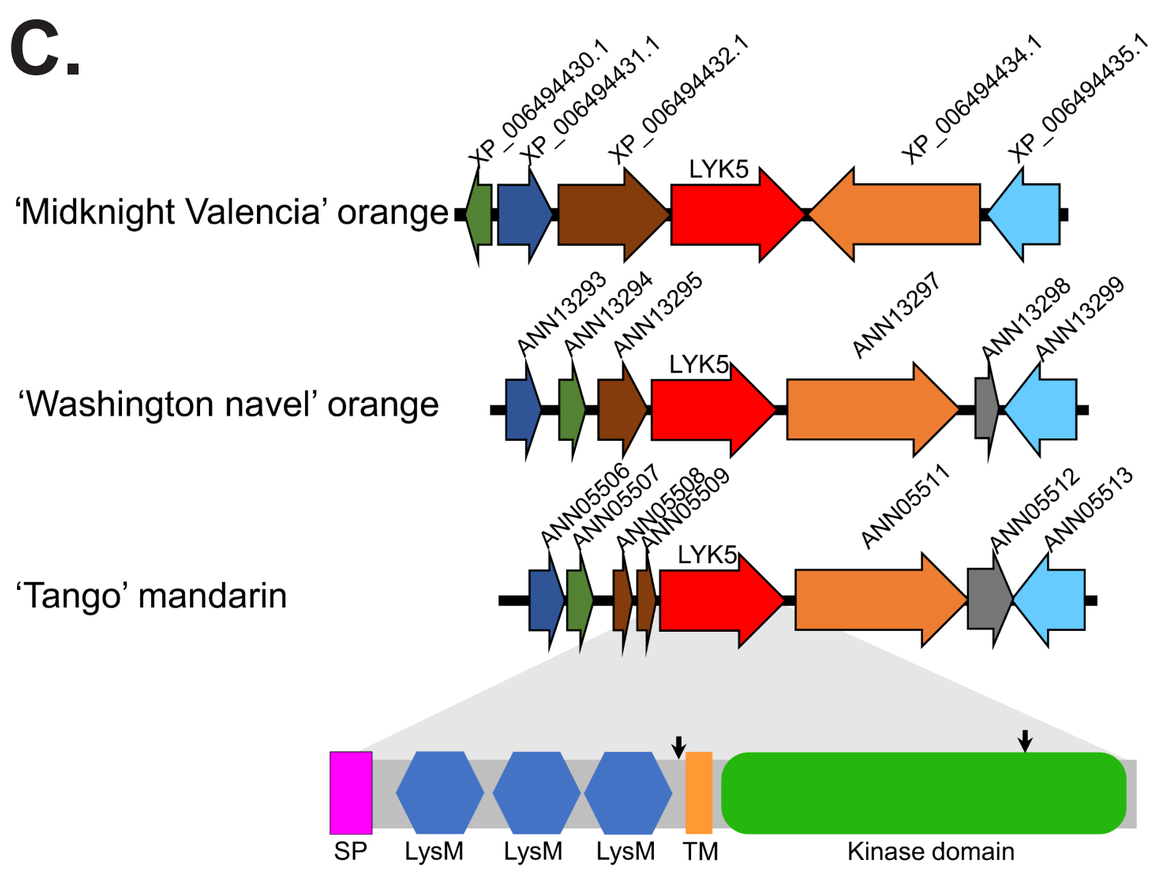

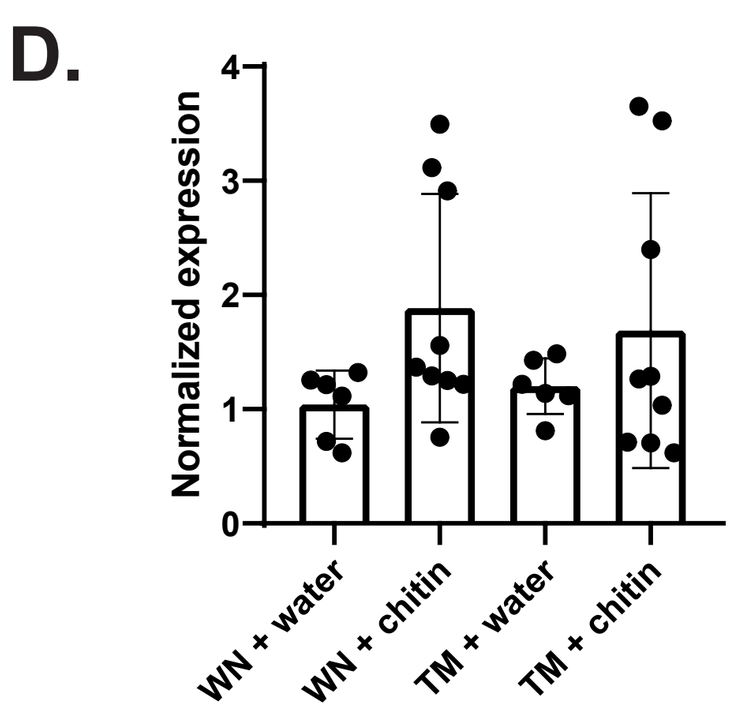

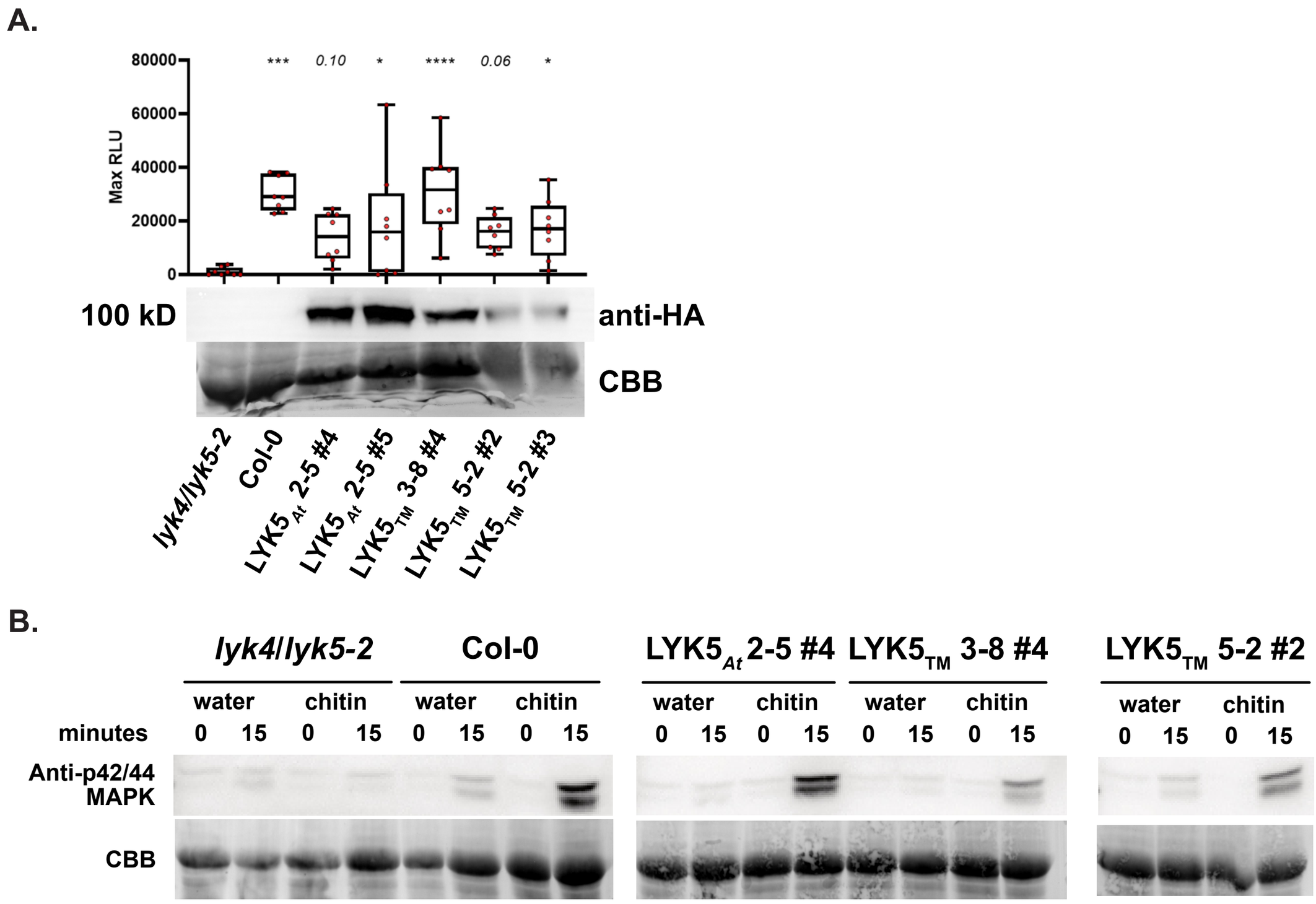

Figure 6. The 'Tango' mandarin LYK5$_{At}$ homolog can complement an *Arabidopsis* chitin perception mutant. A. ROS production of *Arabidopsis lyk4/lyk5-2* knockouts complemented with the indicated *LYK5* constructs after treatment with 10 µM chitin. The bar within the box plot depicts the median of the data, where the box boundaries represent the interquartile range (between the 25th and 75th percentiles) of the data. Box whiskers represent the minimum or maximum values of the data within 1.5x of the interquartile range. Anti-HA-HRP immunoblots visualize the LYK5-HA bands; CBB = Coomassie Brilliant Blue (CBB). Significance of results was determined via ordinary one-way ANOVA, with a post hoc Dunnett's multiple comparison to the *lyk4/lyk5-2* knockout. Asterisks represent significance thresholds: **** = p<0.0001, *** = p=0.0001 to 0.001, ** p=0.001 to 0.01, * p=0.01 to 0.05. B. MAPK induction in response to either water for chitin in *LYK5*-complemented *Arabidopsis lyk4/lyk5-2*, using anti-p42/44 MAPK immunoblotting. CBB = Coomassie Brilliant Blue. All experiments were performed 3 times with similar results.

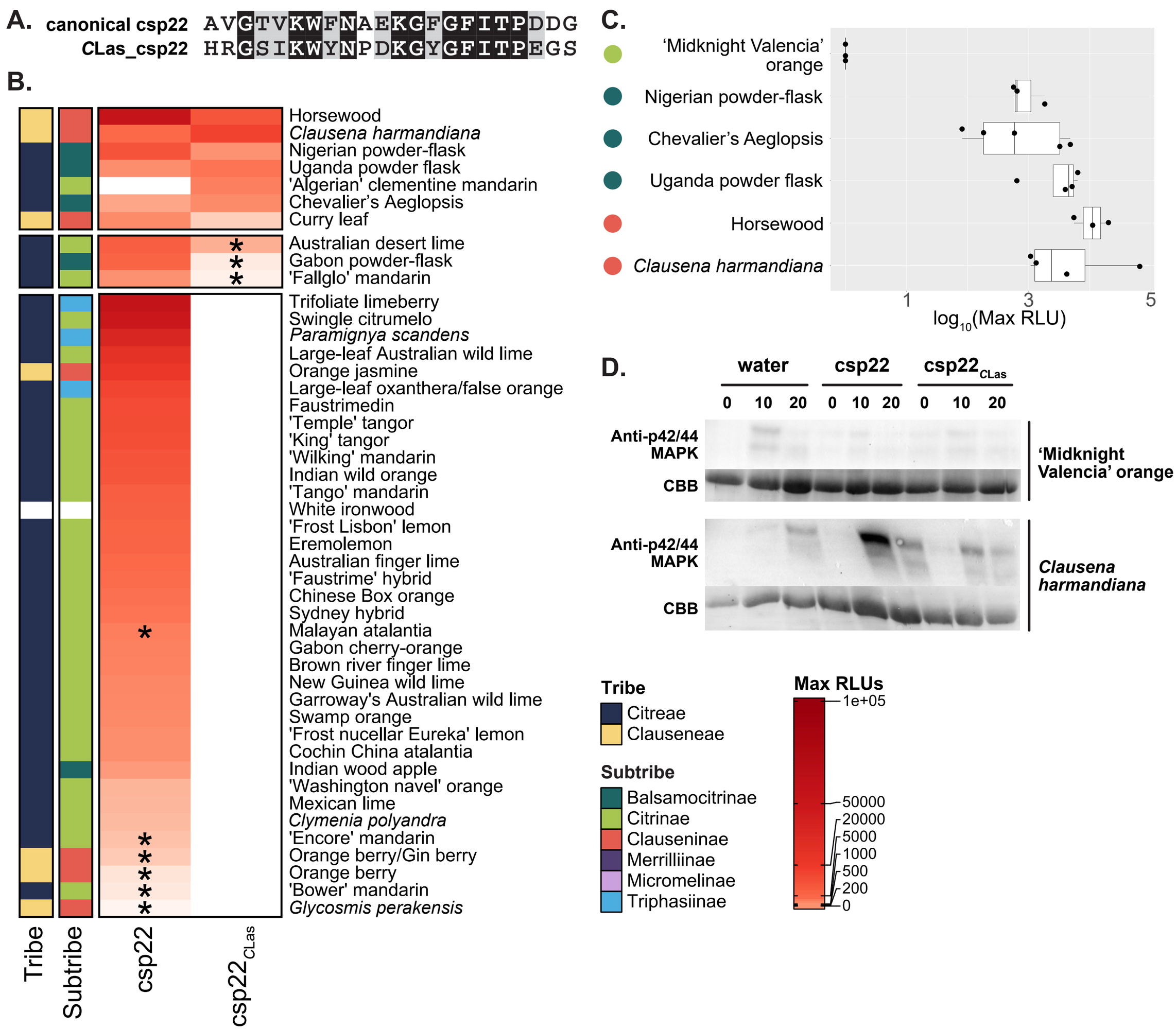

Figure 7. Three Rutaceae subtribes can respond to a polymorphic csp22 from an important citrus pathogen. A. Alignment of the canonical csp22 sequence to the csp22 of *Candidatus* Liberibacter asiaticus ($csp22_{CLas}$). B. Heat map compiling average max relative light units (RLUs) from ROS assays in genotypes within the Rutaceae family, organized by MAMP and phylogenetic relationship. White indicates genotypes in an unresolved tribe. Max RLUs are averages of at least three independent experiments, where *max RLU = (max RLU PAMP – max RLU water)*. <90 RLU is the threshold for no response. Asterisks indicate genotypes that exhibit a variable response, where one or two independent experiments revealed a response. The MAMPs used for treatments are canonical csp22 and csp22 from *Candidatus* Liberibacter asiaticus. C. Box plot of max RLUs for citrus relatives that can respond to 200 nM $csp22_{CLas}$. Max RLUs are averages of at least three independent experiments. Data points on box plots represent the average max RLU for an individual experiment, with n = 8 leaf disks per experiment. The max RLU are plotted on a log10 scale. The bar within the box plot depicts the median of the data, where the box boundaries represent the interquartile range (between the 25th and 75th percentiles) of the data. Box whiskers represent the minimum or maximum values of the data within 1.5x of the interquartile range. D. MAPK induction by csp22 or $csp22_{CLas}$ in either Valencia orange or *Clausena harmandiana*, visualized by p42/44 MAPK antibody immunoblotting. CBB = Coomassie Brilliant Blue.